1975

A Study Of The Interaction Of Acridine Orange With Rat Mast Cells.

Larry Dennis Love
University of Alabama at Birmingham

INFORMATION TO USERS

This material was produced from a microfilm copy of the original document. While the most advanced technological means to photograph and reproduce this document have been used, the quality is heavily dependent upon the quality of the original submitted.

The following explanation of techniques is provided to help you understand markings or patterns which may appear on this reproduction.

1. The sign or "target" for pages apparently lacking from the document photographed is "Missing Page(s)". If it was possible to obtain the missing page(s) or section, they are spliced into the film along with adjacent pages. This may have necessitated cutting thru an image and duplicating adjacent pages to insure you complete continuity.

2. When an image on the film is obliterated with a large round black mark, it is an indication that the photographer suspected that the copy may have moved during exposure and thus cause a blurred image. You will find a good image of the page in the adjacent frame.

3. When a map, drawing or chart, etc., was part of the material being photographed the photographer followed a definite method in "sectioning" the material. It is customary to begin photoing at the upper left hand corner of a large sheet and to continue photoing from left to right in equal sections with a small overlap. If necessary, sectioning is continued again — beginning below the first row and continuing on until complete.

4. The majority of users indicate that the textual content is of greatest value, however, a somewhat higher quality reproduction could be made from "photographs" if essential to the understanding of the dissertation. Silver prints of "photographs" may be ordered at additional charge by writing the Order Department, giving the catalog number, title, author and specific pages you wish reproduced.

5. PLEASE NOTE: Some pages may have indistinct print. Filmed as received.

University Microfilms International
300 North Zeeb Road
Ann Arbor, Michigan 48106 USA
St. John's Road, Tyler's Green
High Wycombe, Bucks, England HP10 8HR

A STUDY OF THE INTERACTION OF ACRIDINE ORANGE WITH RAT MAST CELLS

By

LARRY DENNIS LOVE

A DISSERTATION

Submitted in partial fulfillment of the requirements for the degree of Doctor of Philosophy in the Department of Physiology and Biophysics in The Graduate School of the University of Alabama in Birmingham

BIRMINGHAM, ALABAMA

1975

ACKNOWLEDGMENTS

The author wishes to express sincere appreciation to Dr. S. S. West, Chairman of his graduate committee, for guidance, encouragement, and support throughout the course of this work.

Special thanks are extended to Dr. J. F. Golden for his assistance in obtaining much of the data and to Drs. J. M. Menter, E. M. Weller, S. B. Barker, and L. Rodén for their suggestions, criticisms, and time spent in the review of this research.

The unselfish consideration and encouragement of my wife, Lynda, through these years of graduate study are deeply appreciated.

The major support of this research in the Department of Engineering Biophysics was provided by the National Institute of Dental Research through a Special Research Fellowship.

TABLE OF CONTENTS

Table of Contents (continued)

LIST OF FIGURES

List of Figures (continued)

List of Figures (continued)

LIST OF ABBREVIATIONS AND SYMBOLS

AMPS	Acid mucopolysaccharides
AO	Acridine orange
AO-AMPS	Acridine orange-acid mucopolysaccharides
AO-MC	Acridine orange-mast cell
ATP	Adenosine triphosphate
BPS	Buffered physiological saline
DNA	Deoxyribonucleic acid
g	Gravity
gm	Gram
I_{ex}	Intensity of fluorescence-exciting radiation
I_f	Fluorescence intensity
λ_{ex}	Wavelength of fluorescence-excitation
MC	Mast cell
MSF	Microspectrofluorophotometer
NBS	National Bureau of Standards
pers comm	Personal communication
PMT	Photomultiplier tube
ppu	Phosphor particle units
RNA	Ribonucleic acid
5-HT	5-Hydroxytryptamine

THE MAST CELL

Historical

In 1877, Ehrlich investigated the applicability of some of the then new synthetic dyes for staining histological sections and discovered connective tissue cells which contained granules that not only had an affinity for certain aniline dyes but also tended to produce a shift in the color of the bound dye. He introduced the term "metachromasia" to designate this type of staining and named these cells "mast cells" (MC), because they had the appearance of being well-fed (Ehrlich, 1878). Since their discovery, little has been added to Ehrlich's original morphological description of the MC as observed with the light microscope. The literature concerned with MCs is extremely large and, therefore, only those contributions which were considered the most significant in the development of our knowledge of the cell have been cited in this dissertation.

For approximately 60 years subsequent to the discovery of the MC, the work on this connective tissue element was primarily concerned with its morphology, distribution, staining characteristics, and speculation as to its probable function. This voluminous accumulation of data was comprehensively reviewed by Michels (1938).

From his studies on the staining properties of estersulfate compounds, Lison in 1935 first suggested that metachromatic staining

might have histochemical significance in demonstrating the presence of polymers containing estersulfate groups, such as sulfated polysaccharides (Schubert and Hamerman, 1956). Because of the similarity in staining properties of heparin and MCs with toluidine blue and the close correspondence between the number of MCs present and the heparin content of various tissues, Jorpes, Holmgren and Wilander in 1937 advanced the hypothesis that heparin was contained in MC granules (Jorpes, 1946). It was much later before more direct proof was offered that normal MCs contain heparin (Schiller and Dorfman, 1959).

The MC-heparin hypothesis stimulated new interest, and many investigations were directed toward determining the constituents and function of the cell. Since MCs are frequently observed in the vicinity of small blood vessels, it was first speculated that their function was to produce and liberate heparin which prevented intravascular clotting. Today, there is some doubt as to whether MCs secrete heparin under physiological conditions because, with the exception of the anaphylactic dog, the release of heparin by MCs has not been demonstrated. Heparin may only serve as a structural component in the MC (Lagunoff, 1963).

Following the suggestion that MCs contain heparin, the next important contributions to our understanding of the cell occurred in the 1950s when evidence was presented that they also contain biogenic amines. Riley and West (1953) and Riley (1953) reported finding a relationship between the number of MCs and the histamine content in a variety of normal tissues. Their association of

histamine with the MC has been confirmed by numerous investigators. Representative examples of those are: Cass et al., 1954; Graham et al., 1955; Mota, Ferri, and Yoneda, 1956; and Benditt, 1958. It is well established that factors which produce a degranulation of the cell also elicit a release of histamine (Riley, 1959).

Riley (1959) suggested a possible sequence of events in which both heparin and histamine are utilized to restore the integrity of connective tissue in response to inflammation or injury. He visualized that upon disruption of the MC, histamine is released and rapidly spreads into the surrounding tissue signaling the fibroblast to ingest heparin and heparin granules that are thought to follow the discharge of histamine. Ingested heparin is then converted by the fibroblast into mucopolysaccharide ground substance needed for repair of the acellular connective tissue. In addition, histamine produces a vaso-dilatation of small blood vessels permitting plasma colloids necessary for phagocytosis (Jancsó, Jancsó-Gábor, and Balassy, 1959) to leak into the injured area. Riley's "Mast Cell Cycle" of connective tissue has not been substantiated to any extent by appropriate experiments.

Schayer (1956), using suspensions of rat peritoneal MCs, provided evidence that MCs are capable of synthesizing and storing histamine. He demonstrated that ^{14}C L-histidine was decarboxylated by MCs and also was able to isolate histidine decarboxylase. Benditt (1958) reported the concentration of histamine in isolated MCs is 11 X 10^{-6} gm/mm^3 of cells, or 1.1% of the cell volume.

Benditt and co-workers (1955) chromatographically identified the presence of 5-hydroxytryptamine (5-HT) in pure preparations of normal MCs of the rat. The same cell was later shown to contain 5-hydroxytryptophane decarboxylase, the enzyme necessary for the synthesis of 5-HT and, in addition, pyridoxal-5-phosphate was required as coenzyme. Like both heparin and histamine, 5-HT is located in the cytoplasmic granules (Barrnett, Hagen and Lee, 1958; Hagen, Barrnett and Lee, 1959). 5-HT has been found in MCs of the rat and mouse but appears to be absent in MCs of other species. A close parallelism exists between the number of MCs and the amount of 5-HT present in various tissues (Selye, 1965).

Although I have only alluded to the decarboxylases of the MC, the literature concerned with the rich enzyme pattern of the MC is extensive. Other enzymes reported to be contained in MCs are chymase, tryptase, fibrinolysin, hydroxylases, β-glucuronidase, dehydrogenase, esterases, monoamine-oxidase, phosphatidase, phosphatase, ATP-ase and diaphorase (Selye, 1965).

The rat MC granule was characterized by Lagunoff et al. (1964), using biochemical techniques, and was found to contain heparin, histamine, and chymase. On a dry weight basis, heparin constituted 30%, basic protein 35%, phospholipid less than 2%, and histamine approximately 10%. Uvnäs, Åborg, and Bergendorff (1970) reported the heparin:protein ratio in the rat MC granule to be 1:2.5.

The exact structural relationship between heparin, protein, and the amines present in MC granules is not known. It is speculated by some that the granule is a heparin-protein complex formed

by ionic interaction between sulfate groups on heparin and cationic amino groups on the protein, and amines and possibly other cations are bound electrostatically to the complex (Lagunoff et al., 1964; Åborg, Novotný and Uvnäs, 1967; Åborg and Uvnäs, 1968; Uvnäs, Åborg and Bergendorff, 1970; Bergendorff and Uvnäs, 1972). Other investigators, from their studies on heparin obtained from pig intestinal mucosa, suggest that heparin in the native state is bound covalently to protein by a galactosylxylosylserine linkage (Lindahl et al., 1965; Lindahl and Rodén, 1965; Lindahl, 1966).

Polysaccharides of Mast Cells

Oliver, Bloom, and Mangieri (1947) fractionated heparin from dog MC tumors and reported that the heparin content varies with the degree of anaplasia. Since that time, a great deal of effort has been directed toward determining if other polysaccharides are also present in MCs.

The correlation between the number of MCs present in a tissue and its hyaluronic acid content prompted Asboe-Hansen (1949) to advance the hypothesis that hyaluronic acid in mesenchymal tissue is produced by MCs. He noted that MC granules stain like hyaluronic acid, and where hyaluronic acid is found, the number and size of MCs are increased. This hypothesis stimulated additional investigations which have not entirely substantiated his speculations.

A number of histochemical studies have suggested that MCs contain mucopolysaccharides other than heparin. Fullmer (1959)

incubated MCs with glucuronidase and reported their staining characteristics could be attributed to the selective removal of a mucopolysaccharide substance(s). Winkelmann (1959) also noted different staining affinities of night blue (an orthochomatic stain not normally used to stain mast cells) between the MCs of the rat, mouse, and hamster. No basis for the variable staining capacity of MC granules of these species was apparent; however, this experiment suggested that a difference in sulfated mucopolysaccharides or heparinoid substances might be responsible.

The histochemical work of Velican and Velican (1959) on human MCs was in agreement with the views of Asboe-Hansen with regard to the presence of hyaluronic acid. The investigation employed toluidine blue to show the effect of hyaluronidase on the cytoplasmic granule; the metachromatic content disappeared completely in approximately 15% and partially in 36.5% of the cells after treatment with hyaluronidase. These results were interpreted by the authors to mean that the metachromatic content of certain cells is composed entirely of hualuronic acid, while in others it forms only a portion of the metachromatic material.

Using alcian blue with a safranin counter stain, Worthington and Bailey (1962) found MCs to show much variation in the staining reaction. Some cells contained mixtures of red, blue, and orange-red granules. Horsfield (1966) utilizing the same stain studied the staining properties of both fixed and unfixed rat mesentery MCs as a function of pH, paraffin embedding medium, and also vitamin C, tetracycline, and hyaluronidase treatments. From the metachromatic

staining characteristics, he concluded that MCs contain a number of mucopolysaccharides in addition to heparin.

Questions concerning the presence of mucopolysaccharides other than heparin also developed from early chemical analyses of MC tumors and normal MCs. Magnusson and Larsson (1955) used $^{35}SO_4$ to label polysaccharides in dog MC tumors. Their findings indicated the presence of a galactosamine constituent in addition to heparin. Korn (1958) in a similar experiment also isolated a crude chondroitin sulfate fraction from mouse mastocytoma. However, Schiller and Dorfman (1959) analyzed rat MCs obtained from peritoneal washings and, by paper chromatography, found heparin to be the only mucopolysaccharide present. The absence of other polysaccharides was explained on the basis that they possibly resulted from connective tissue contaminants in preparations from solid tumors.

Ringertz (1960) explored the acid mucopolysaccharides in ascites sublines of the Dunn and Furth transplantable MC tumors. This investigation was undertaken to determine if the main polysaccharide components in solid tumors originated from tumor cells or from connective tissues. The complex chromatographic patterns of the solid tumors and their ascites sublines were the same, suggesting the major portion of non-heparin polysaccharides was contributed by tumor cells rather than by other tissues present in solid tumors. Analytical data on the polysaccharide fractions revealed a heparin-like material with a low sulfate content, chondroitin sulfate, and heparin. Chemical analysis of the unfractionated polysaccharides from the Furth and Dunn mastocytomas

showed galactosamine accounted for 20-40% and 24%, respectively, of the amino sugars; glucosamine made up the remainder. In a similar study on the normal rat peritoneal MC, heparin was the only polysaccharide identified (Bloom and Ringertz, 1960).

Brunish and Asboe-Hansen (1965) found galactosamine to constitute 19.1% of the total hexosamine in Rask-Nielsen transplantable mastocytomas. Their findings were in agreement with those of Ringertz (1960) and were based on the analysis for glucosamine and galactosamine content before and after the fractions were treated with hyaluronidase. Heparin or its precursor comprised 39% of the acid mucopolysaccharides, 42% was thought to be hyaluronic acid, and the balance was chondroitin sulfates.

Although the previously cited histochemical studies presented evidence suggesting polysaccharides other than heparin as possible components of normal MCs, a lack of supportive chemical characterization persisted until methods (Barker, Cruickshank, and Webb, 1965a, b) were developed which permitted the separation and identification of mucopolysaccharides in small volumes of material. A number of mucopolysaccharides in normal MCs from the rat peritoneal cavity have been identified by Horsfield and Summerly (1966). The cells were incubated in a culture medium containing $^{35}SO_4$ and ^{14}C-glucose which were incorporated into the mucopolysaccharides later separated by column chromatography. The sulfate labeled material had peaks of activity corresponding to the elution positions of chondroitin-4-sulfate, chondroitin-6-sulfate, dermatan sulfate, and heparin reference samples; and also a peak which was

thought to represent keratan sulfate. The glucose labeled fractions contained a compound that was eluted at the position for hyaluronic acid (Barker, Cruickshank and Webb, 1965a). The unusually broad elution peak for chondroitin-4-sulfate was resolved into two peaks after labeling. This was interpreted by the authors to indicate the presence of heparitin sulfate which has an elution position close to that of chondroitin-4-sulfate. The type of experiment conducted by Horsfield and Summerly did not permit the quantitation of the mucopolysaccharides that were identified, and their work has not been confirmed by other investigators.

One can conclude that in the normal MC of the rat, heparin is the major, if not the only, polysaccharide present. Heparin, a sulfated high molecular weight polymer, is thought to consist of alternating residues of uronic acid and glucosamine, and contains various proportions of O-sulfate, N-sulfate, and N-acetyl groups. The uronic acid components of the polymer have been identified as L-iduronic and D-glucuronic acids (Cifonelli and Dorfman, 1962). The exact structure of heparin, the most powerful chromatrope of animal origin (Schubert and Hamerman, 1956), is not known since its composition appears to vary as a function of source, sample purity, and methods used for structure determinations. Helting and Lindahl (1971) have proposed a tetrasaccharide repeat unit for heparin depicted in Figure 1.

FIGURE 1

Proposed structure of heparin tetrasaccharide repeat unit containing both iduronic and glucuronic acid.

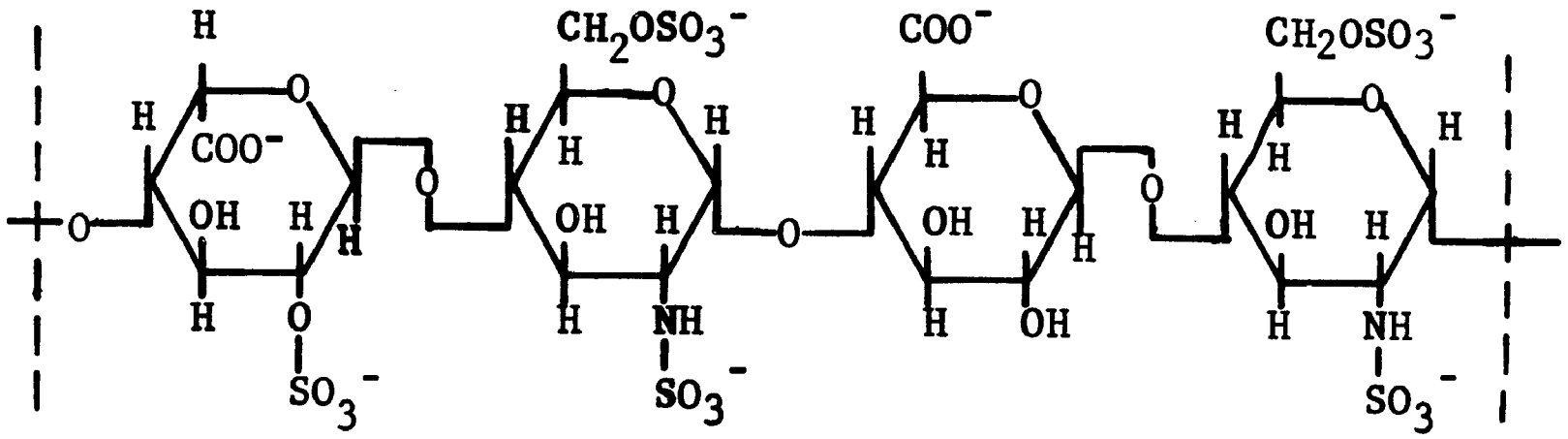

Conclusions

The MC continues to engage the attention of many investigators. Originally, no sound basis existed for ascribing any real function to the cell. Today, it remains an enigma because of the many and apparently unrelated functions attributed to it.

Histochemical and biochemical investigations have greatly contributed to our knowledge of the MC by showing it to contain a number of potent biological substances. Now, there is general agreement that MCs contain and produce heparin, histamine, and a variety of enzymes, and therefore are possibly involved in important pharmacological functions associated with inflammation, antithrombic activity, hypersensitivity reactions (anaphylaxis), wound healing, fat metabolism, and calcification. However, among the many suggested functions of the MC, none has been documented with sufficient experimental evidence and the exact role of the MC in physiological and pathological processes is still unresolved (Padawer, 1970).

PURPOSE OF THIS STUDY

The long term goal of this research is directed toward understanding the MC by studying it in a viable condition and is based on the premise that data which describe the phenomenological behavior of a chemically identified intracellular component will provide means for gaining insight into the nature and function of the cell. More specifically, this investigation is concerned with the necessary first step, namely, identifying some intracellular component(s) of the MC by a means which permit the cell to maintain its morphological and functional integrity and characterizing the MC as a function of experimental changes by measuring the accompanying changes which occur in the identified intracellular constituent.

In essence, this approach differs from that most frequently used in histochemistry and biochemistry in that cells in the living state are utilized rather than cell extracts of fixed preparations. There are certain restrictions on experimental methods employed in obtaining chemical information from an intracellular constituent of a living cell. The techniques must not interfere appreciably with the physiology of the cell, and it is desirable for cell data to be in a form which permits their comparison with solution data from well characterized biomolecules. Biophysical cytochemistry provides

us with the necessary nondestructive physical-chemical techniques for experiments of this nature.

BIOPHYSICAL CYTOCHEMISTRY

Biophysical cytochemistry employs physical optical and physical chemical methods to examine microscopic material and obtain chemical information from it. These techniques are useful for studying intracellular constituents of living cells and do not produce noticeable alterations in either cell morphology or function.

The spectroscopic methods most commonly used in this laboratory involve the use of fluorescent vital dyes which, when complexed with a substrate, exhibit characteristic alterations in optical properties. The alterations in optical properties can provide information about the nature of the substrate at the molecular level. Therefore, such vital dyes can be referred to as molecular probes and have the potential to be useful in studying biomolecules both in their native environment and in solution.

For the present investigation, acridine orange (AO) was selected from among the large number of fluorescent vital dyes because its spectral properties in aqueous solutions have been characterized by Zanker (West, 1969), and because other studies in this laboratory using AO as a fluorescent molecular probe afforded a means for comparison. AO, a small, planar, dye molecule exists as a totally dissociated cation at physiological pH ($\simeq$ pH 7). The structure of one of its three resonating forms is shown below.

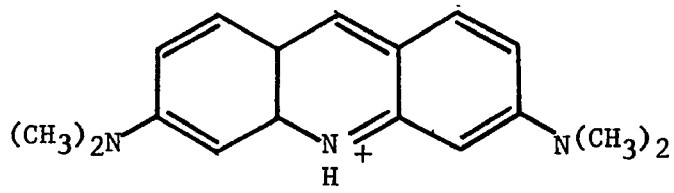

The optical properties of the dye are a function of its concentration and other environmental factors, such as pH, solvent, ionic strength, binding substrate, etc. Since the small amount of dye required for staining is nontoxic to the cells, it can be used as a vital stain (DeBruyn, 1950; Hill, Bensch and King, 1959).

In 1952, Zanker studied the absorption and fluorescence spectra of AO as a function of concentration, Figures 2 and 3, and found the dye in aqueous solution to exist in two forms (West, 1969). A monomeric species is found at low dye concentrations and is characterized by an absorption band with a peak at 492 nm and an emission band at 540 nm. At high dye concentrations, the dye forms dimers and higher polymers. In the aggregated state, the absorption maximum appears at 448 nm and the corresponding emission maximum at 660 nm.

Metachromatic behavior, similar to that of AO in aqueous solution, is observed in certain AO-polymer complexes. Steiner and Beers (1959) and Bradley and Wolf (1959) have proposed two types of binding models for AO-polymer complexes. In their terminology, Complex II corresponds to the monomeric species, and Complex I forms with increasing dye to polymer ratios resulting in dye-dye interaction.

The use of AO as a fluorescent biological stain for both fixed and supravital microscope preparations has been extensively reviewed

FIGURE 2

Absorption spectra of acridine orange in aqueous solution. Solvent: citrate-phosphate buffer, pH 6.0, 20°C. (From Zanker, 1952, cited by West, 1969).

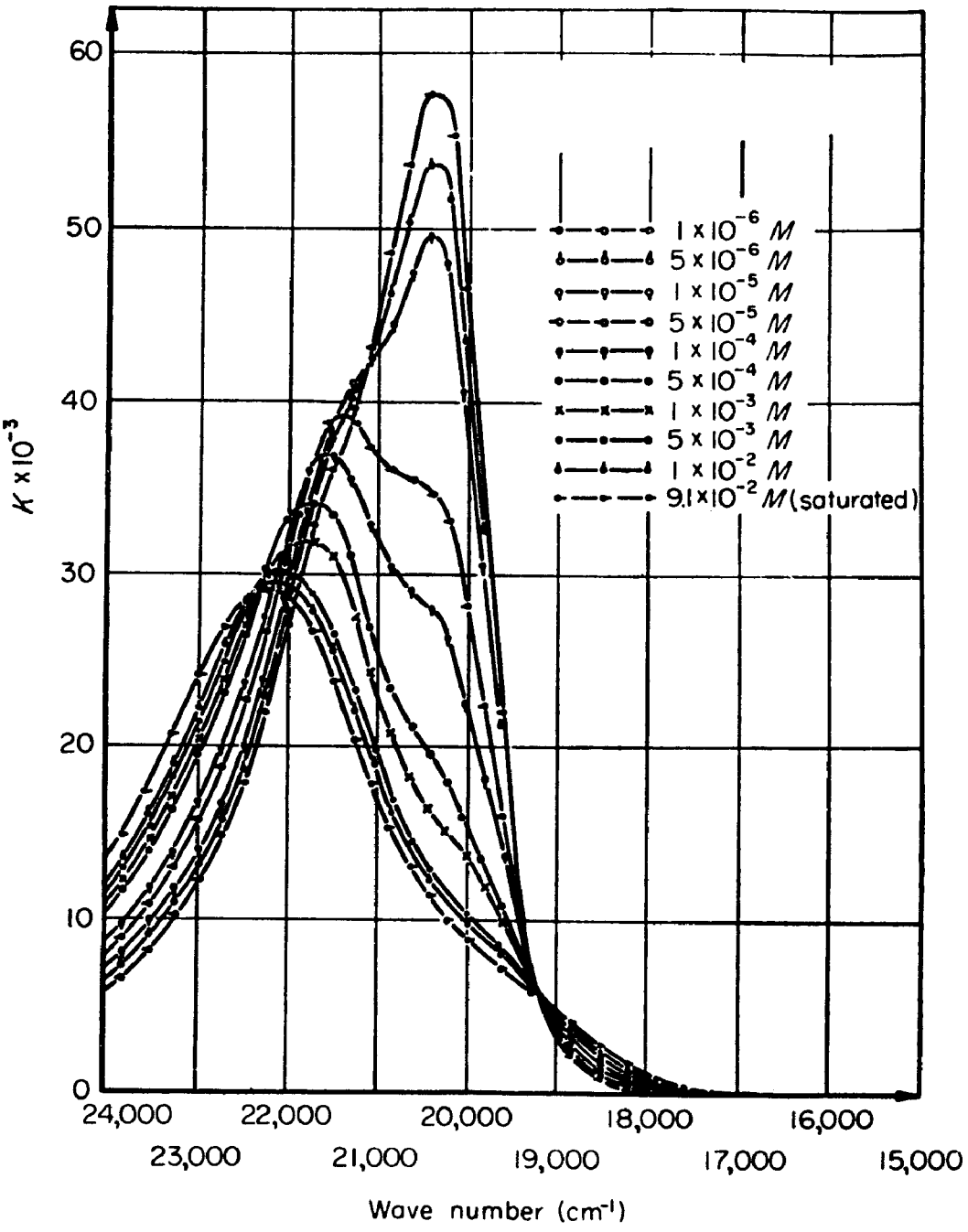
60
50
40
30
20
10
0
K x10^-3
1 x10^-6 M
5 x10^-6 M
1 x10^-5 M
5 x10^-5 M
1 x10^-4 M
5 x10^-4 M
1 x10^-3 M
5 x10^-3 M
1 x10^-2 M
9.1x10^-2 M (saturated)
24,000
23,000
22,000
21,000
20,000
19,000
18,000
17,000
16,000
15,000
Wave number (cm^-1)

FIGURE 3

Normalized fluorescence emission spectra of acridine orange in aqueous solution. Solvent: citrate-phosphate buffer, pH 6.0, 20°C. (From Zanker, 1952, cited by West, 1969).

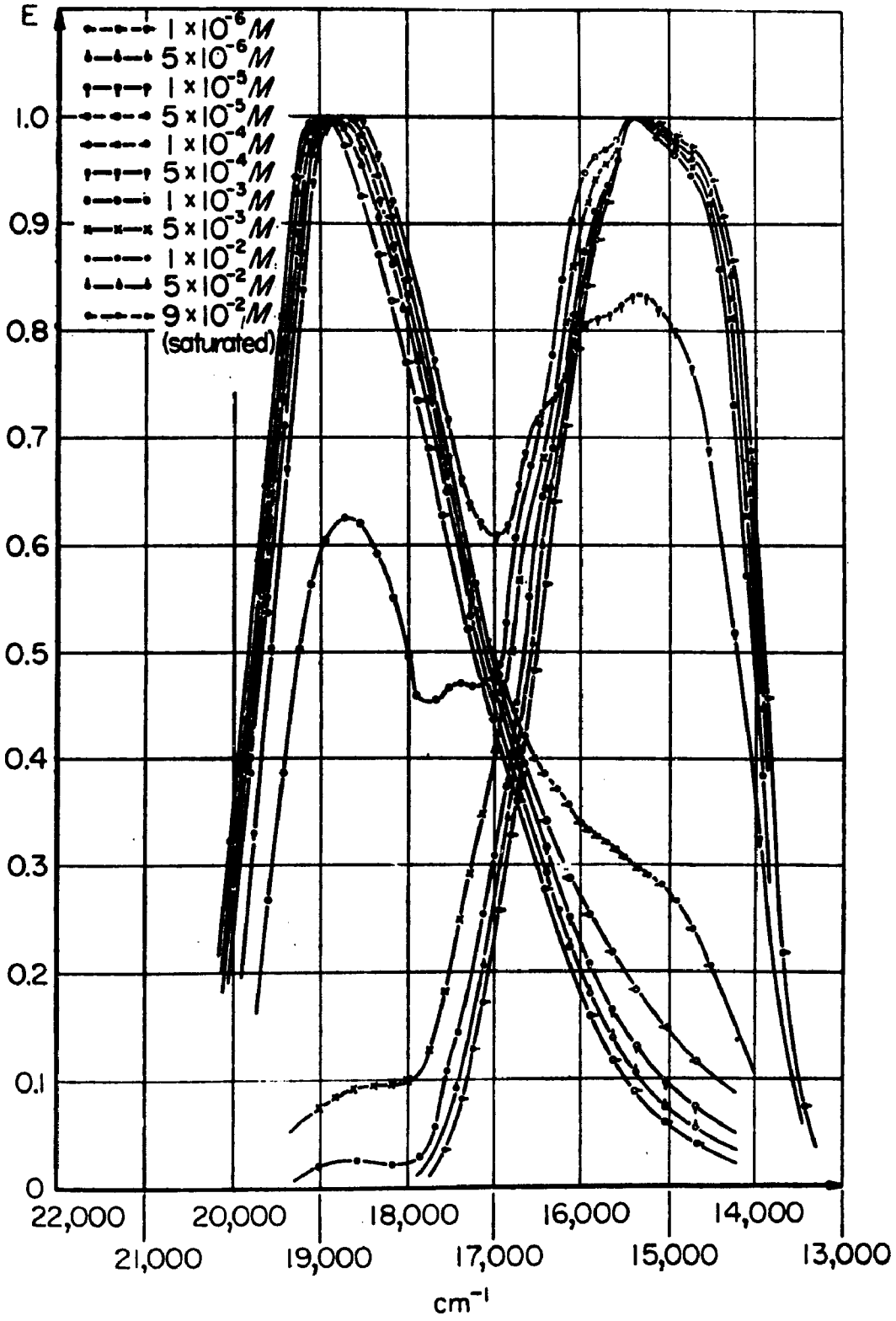
E
1 x 10⁻⁶ M
5 x 10⁻⁶ M
1 x 10⁻⁵ M
5 x 10⁻⁵ M
1 x 10⁻⁴ M
5 x 10⁻⁴ M
1 x 10⁻³ M
5 x 10⁻³ M
1 x 10⁻² M
5 x 10⁻² M
9 x 10⁻² M
(saturated)
1.0
0.9
0.8
0.7
0.6
0.5
0.4
0.3
0.2
0.1
0
22,000
21,000
20,000
19,000
18,000
17,000
16,000
15,000
14,000
13,000
cm⁻¹

by Price and Schwartz (1956), Bertalanffy (1963), and West (1969). Although AO has been used primarily in a qualitative manner for staining fixed material, it can be used to obtain quantitative chemical information about the substrate with which it complexes. A fluorescence microspectrophotometric technique has been developed for obtaining spectrochemical data from cells that have been quantitatively stained (Loeser et al., 1960; Loeser and West, 1962; West, 1965, 1969). Quantitative staining refers to a cell staining technique which permits the calculation of the average amount of dye taken up per cell for a population of cells. The sensitivity of fluorescence measurements makes it possible to record fluorescence emission spectra from individual cells containing as little as approximately 1 X 10^{-18} mole AO.

It is imperative that spectra be corrected to remove any distortions produced by the instrument (e.g. photomultiplier tube (PMT) sensitivity and transmission characteristics of the various optical components). Only then can fluorescence spectra serve to identify the intracellular substrate complexing with the dye and a valid comparison of spectral data be made with other cytochemical and <u>in vitro</u> solution studies. The microspectrophotometric technique also provides for visual examination of the intracellular-dye complex and relates the data obtained from quantitative staining and corrected spectra to cell type and localization within the cell. Equilibrium binding parameters obtained from biophysical cytochemical studies on AO-nucleic acid complexes in the supravitally-stained

leukocyte (West, 1965, 1969) have correlated well with studies of AO-nucleic acid complexes in solution (Ichimura et al., 1969).

The biophysical cytochemical spectroscopic methods, microspectrofluorophotometry and microspectropolarimetry, have been described in detail elsewhere (West, 1965, 1969, 1970). Both techniques are useful for studying intracellular constituents; however, only microspectrofluorophotometry was used in this investigation.

MATERIALS AND METHODS

Buffered Saline Solution

A buffered physiological saline (BPS) solution, pH 7.0, was used as the solvent for all serial dye dilutions and also served as a suspending medium for cells. It was prepared with McIlvaine's citrate-phosphate buffer (Hodgman, 1954) by first adding 20 ml of the phosphate solution to a liter of 0.154 M NaCl which produced a pH slightly higher than desired. Approximately 4 ml of the citrate solution were then added to adjust the saline solution to pH 7.0 and to provide some buffering capacity. The molarity of the buffer solution was approximately 0.004.

Acridine Orange Solutions

The purified AO used in this study was generously supplied by Dr. Julian Menter. Deionized water was used as the solvent for the concentrated stock dye solution (1.1×10^{-3} M) from which dilutions were made for all experiments. Concentration of the stock solution was determined by absorption spectroscopy of dilutions of the stock solution in ethanol and was found to remain stable during the course of this investigation. The stock solution was stored in low actinic glassware at $4^{o}C$.

BPS was the solvent used for making serial dye dilutions from the stock solution. Serial dilutions from 5.5 X 10^{-5} M to 5.5 X 10^{-8} M were prepared for each experiment. The fluorometer was used to check the accuracy of each dilution according to the technique described by West (1969).

Cell Preparations

Normal MCs were obtained from the peritoneal cavities of adult male Sprague-Dawley rats (Southern Animal Farms, Inc., Prattville, Alabama) weighing 300 to 400 gms. The animals were sacrificed by putting them into a 3,000 ml beaker which was then filled with CO_2. The abdominal skin was removed and a small midventral incision, approximately 4 mm, was made into the peritoneal cavity. Approximately 25 ml of BPS were pipetted into the peritoneal cavity and the incision was held closed with tissue forceps while the abdomen was gently massaged with the fingers for 90 seconds. The incision was then extended to provide access for aspirating the peritoneal washings with a large medicine dropper.

The pooled washings from several animals were filtered through a stainless steel millipore filter support screen (Millipore Corp., Bedford, Massachusetts, Cat. No. XX20 04708) to remove pieces of fatty tissue and hairs which were sometimes present. The filtered cell suspension was centrifuged (I.E.C. HN-S Centrifuge) at 130 X g for 8 min. The supernatant was decanted, and the cell pellet was resuspended in 4 ml of BPS.

MCs were separated from other cells present in the peritoneal washings following generally the method of Lagunoff (1972). The cell suspension was layered over 5 ml of a 35% albumin preparation (Pathocyte-4, Miles Laboratories, Kankakee, Illinois), specific gravity 1.10, in a 15 ml round bottom test tube. The tube was centrifuged for 20 min at 220 X g. MCs entered the albumin leaving the other cells at the albumin-saline interface. The nonsedimenting cells and saline suspending medium were aspirated with a disposable pipette. The albumin containing the MCs was diluted with 6 ml of BPS and centrifuged for 10 min at 130 X g. The supernatant was decanted and the MCs were resuspended in BPS to a final concentration of approximately 4.0 X 10^5 cells per ml as determined with a hemacytometer. No effort was made to completely remove all albumin by washing since small amounts of albumin had the beneficial effects of preventing clumping and disintegration of the cells. All steps in the MC preparation were done at room temperature.

Quantitative Staining of Mast Cells

A 1.0 ml aliquot of the cell stock suspension containing approximately 4 X 10^5 cells was placed in each staining tube, a 12 X 75 mm Pyrex test tube. The staining tubes were centrifuged at 80 X g for 6 min, the supernatants decanted, and the sedimented cells resuspended in 2.0 ml of AO staining solution. Since glass has a slight binding affinity for AO, a control tube was prepared for each concentration of AO used. The control tube, also a

12 X 75 mm Pyrex test tube, contained no cells, only AO solution of the same concentration and volume used in the cell staining tube. The staining tubes were sealed with parafilm® and inverted every 15 min while staining to keep the cells in suspension.

After the staining reaction had reached equilibrium (approximately 45 min at room temperature), a 0.5 ml aliquot of the cell staining suspension was removed for making cell counts and fluorescence measurements on single cells. The cells in the staining suspensions were pelleted by centrifugation and the quantity of dye remaining in the decants was determined by fluorescence emission at 540 nm as measured with the fluorometer.

Fluorescence Measurements

Instrumentation

The microspectrofluorophotometer (MSF) (Golden and West, 1974), was designed and built in this laboratory for the purpose of rapidly recording fluorescence emission spectra of microscope slide preparations of biological material or of solutions contained in cuvettes that can be placed on the microscope stage. The MSF has the capability to record the spectrum between 400 nm and 700 nm in 0.6 second; the rapid scanning feature is particularly useful in making measurements on material that is photolabile.

Figure 4 is a block diagram showing the basic components of the MSF consisting of a light microscope equipped with a photometric optical train, a rapid scanning monochromator, and associated

FIGURE 4

Block diagram of the microspectrofluorophotometer.

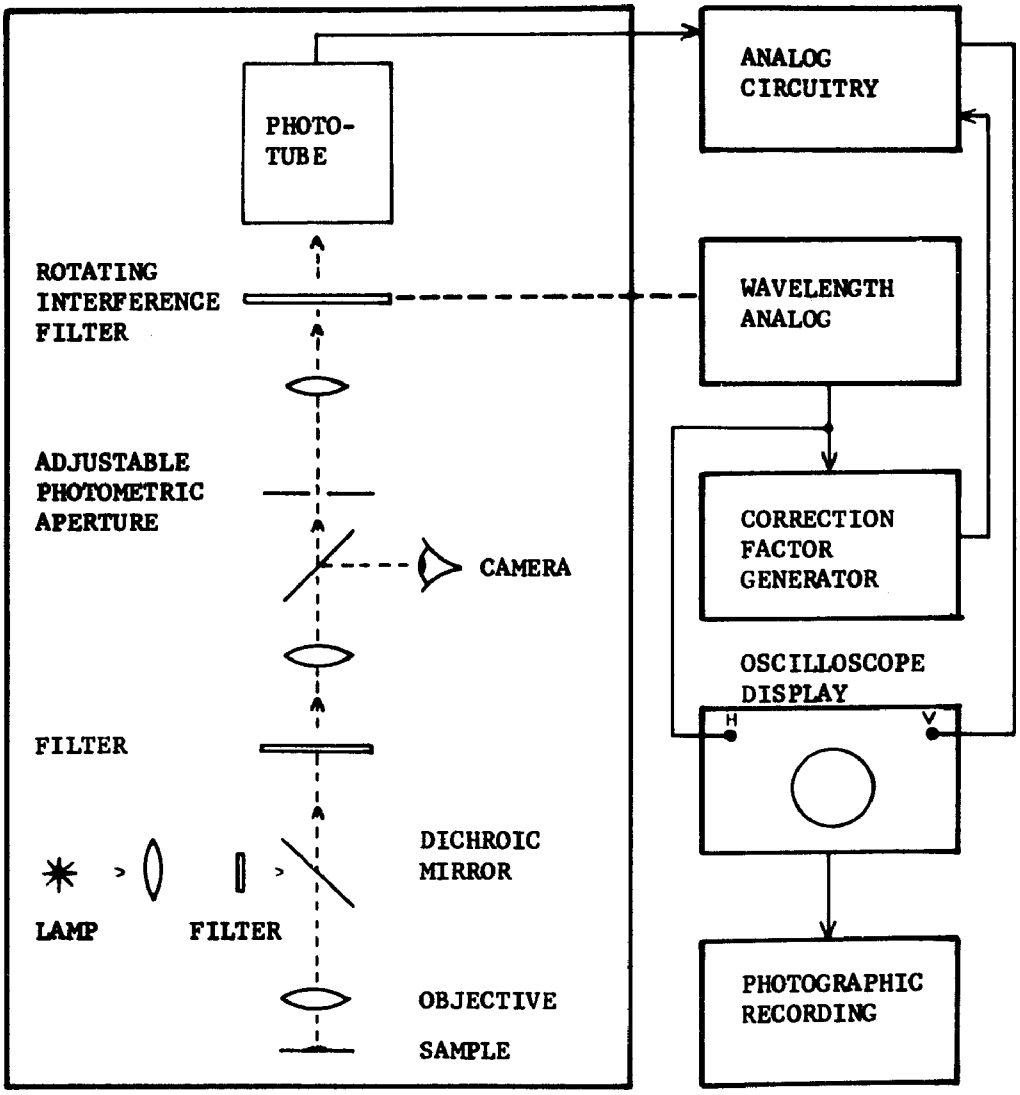
ANALOG CIRCUITRY
PHOTO-TUBE
ROTATING INTERFERENCE FILTER
WAVELENGTH ANALOG
ADJUSTABLE PHOTOMETRIC APERTURE
CAMERA
CORRECTION FACTOR GENERATOR
OSCILLOSCOPE DISPLAY
H
V
FILTER
DICHROIC MIRROR
LAMP
FILTER
OBJECTIVE
SAMPLE
PHOTOGRAPHIC RECORDING

instrumentation to produce corrected fluorescence emission spectra on-line. The light microscope is a Leitz Orthoplan equipped with a Ploem type epi-illumination system which is normally used for fluorescence measurements, and a transmitted light Smith interference contrast imaging system. The latter system is not shown in the diagram.

Fluorescence emitted by the sample is collected by the objective and passes through a barrier filter selected to remove undesired radiation. The fluorescence emission to be analyzed passes next through an adjustable photometric aperture which was positioned in the image plane and included in the optical train (Leitz MPV1) to the scanning monochromator located in the plane of the eyepoint. The scanning monochromator consists of a rotating linear-interference wedge (Barr and Stroud, Ltd., Glasgow, Scotland) with a half-value bandwidth of approximately 15 nm. Radiation transmitted by the wedge is detected by a PMT (EMI type 95580A), the output of which is corrected on-line for all spectroscopic distortions produced by the optical system and the phototube. The vertical oscilloscope input signal corresponds to the corrected PMT signal (intensity of fluorescence emission) and a linear potentiometer mechanically coupled to the rotating interference wedge supplies the voltage which drives the horizontal sweep. The oscilloscope display of the corrected fluorescence emission versus wavelength and the reference information needed for subsequent processing of the data are recorded on 35 mm film with a Beattie-Coleman camera (Coleman System, Irvine, California).

The optical system in the MPV1 enables the superposition of the image of the adjustable photometric aperture on the image of the microscope field. The combined image may be photographed to record that portion of the field selected for measurement. This feature is extremely useful when only certain morphological constituents within an intact cell are to be analyzed.

The rotating interference wedge used as a scanning monochromator can be switched to a stationary mode instead of a scanning mode. This permits the wedge to be stopped at a particular wavelength, and the MSF can be set to record the temporal behavior of fluorescence at that wavelength.

Fluorescence-exciting radiation was provided by a 100 watt high pressure mercury arc lamp (Illumination Industries, Sunnyvale, California, Cat. No. 112-2118) and a special power supply constructed in this laboratory (West, 1969). This combination provided a stable source of radiation which varied no more than 3% over 13 hours. A Ditric narrow-band 3-cavity interference filter (Ditric Optics, Marboro, Massachusetts) was used to isolate a particular spectral line of mercury as the source of fluorescence-exciting radiation. This type of filter has sharp cut-off transmittance characteristics; thus, radiation outside the passband is effectively blocked. For fluorescence spectra measurements, 436 nm was the wavelength of fluorescence-exciting radiation. When the intensity of fluorescence emission at 660 nm was measured as a function of time, the wavelength of fluorescence-excitation was 546 nm to avoid excitation of the green spectroscopic species.

A barrier filter was placed in the tube of the microscope before the PMT to absorb stray fluorescence-exciting radiation. Leitz K470 and K580 barrier filters were used with fluorescence-excitation at 436 nm and 546 nm, respectively.

Fluorescence Standard

The MSF can not measure fluorescence intensity in terms of absolute units of radiation without a suitable standard. Therefore, a zinc cadmium sulfide phosphor particle (NBS Standard Sample 1023*), permanently mounted on a microscope slide, was used as an arbitrary fluorescence standard (Golden and West, 1974). The phosphor particle was used to calibrate fluorescence intensity in phosphor particle units (ppu) which are related to absolute units of energy by a constant.

Fluorescence properties of the phosphor particle are such that, for a given wavelength of fluorescence-excitation, a constant fluorescence emission spectrum is observed, and the amplitude of emission is directly proportional to the intensity of fluorescence-exciting radiation (I_{ex}).

A corrected fluorescence emission spectrum of the phosphor particle was recorded at the beginning and end of each experiment. Thus, the phosphor particle standard provided not only a basis for comparing fluorescence intensities but also a means to check the performance and spectroscopic properties of the system.

---

* Luminescence properties not specified by NBS.

Procedure for Obtaining Corrected Fluorescence Emission Spectra

When the object of interest was in focus and centered on the microscope stage, the variable photometric aperture was reduced to encompass and isolate it for measurement. The room was made dark to reduce stray radiation and possible damage to the sensitive PMT during measurements. The MSF was switched to the fluorescence mode. The sample was irradiated with fluorescence-exciting light (436 nm) and, immediately thereafter, with the oscilloscope camera set for multiple exposures, a photograph was taken of the oscilloscope display of the corrected fluorescence emission spectrum.

Additional reference information (background spectrum, wavelength calibration points, and amplitude calibration lines) required for subsequent processing and analysis of the data was recorded on each film frame containing an emission spectrum. After recording the spectrum and before readjusting (refocussing, changing aperture size, etc.) the MSF, the feature of interest was moved out of the photometric aperture, and a corrected fluorescence emission spectrum was recorded of the background (area in the field immediately adjacent to that feature). Next, 546 nm and 691 nm mercury lines which served as wavelength calibration points were recorded on the film frame by photographing the oscilloscope display of the spectral transmittance of narrow-band interference filters which transmit maximally at these wavelengths. With the oscilloscope camera set in the film transport mode, the last information put on the data frame was a 1.0 cm vertical amplitude trace which served as a reference in measurements of the amplitude of fluorescence emission.

The wavelength calibration information was utilized in data processing to align the film in the photographic process in which paper was twice exposed; once to expose the mercury spectral lines, once again to record the corrected emission spectra in proper register with the mercury lines used for wavelength calibration. Figure 5 is an example of the raw data in the form of a photograph. Using this photograph, the background spectrum was subtracted from that of the feature of interest, because the amplitude of fluorescence of the feature, as recorded, also contained some contributions from the background. The 0.1 cm calibration lines provided a scale factor for measuring the amplitude of fluorescence intensity in ppu with due consideration given to PMT excitation and oscilloscope scale factors.

Fluorescence Emission Spectra from Single Cells

Cell preparations for fluorescence spectra were made by removing a drop of the cell staining suspension and placing it on a glass microscope slide. A coverslip was placed over the drop and sealed to the slide by the application of hot paraffin wax to the edges. The slide was examined visually in the MSF using Smith interference contrast in tungsten light. A yellow filter (Corning 3484) was placed in the light path between the lamp and sample to avoid fluorescence excitation.

After isolating a cell for measurement, the MSF was switched to the fluorescence mode, and a corrected fluorescence emission spectrum recorded of the cell. Only one spectrum was recorded per

FIGURE 5

Photograph of the oscilloscope display of corrected fluorescence emission spectra in register with the calibrated wavelength scale.

A, corrected spectrum of a mast cell plus background; B, 546 nm mercury line calibration points; C, 691 nm mercury line calibration point; D, 1.0 cm amplitude calibration lines; E, corrected background spectrum. λ_{ex} = 436 nm.

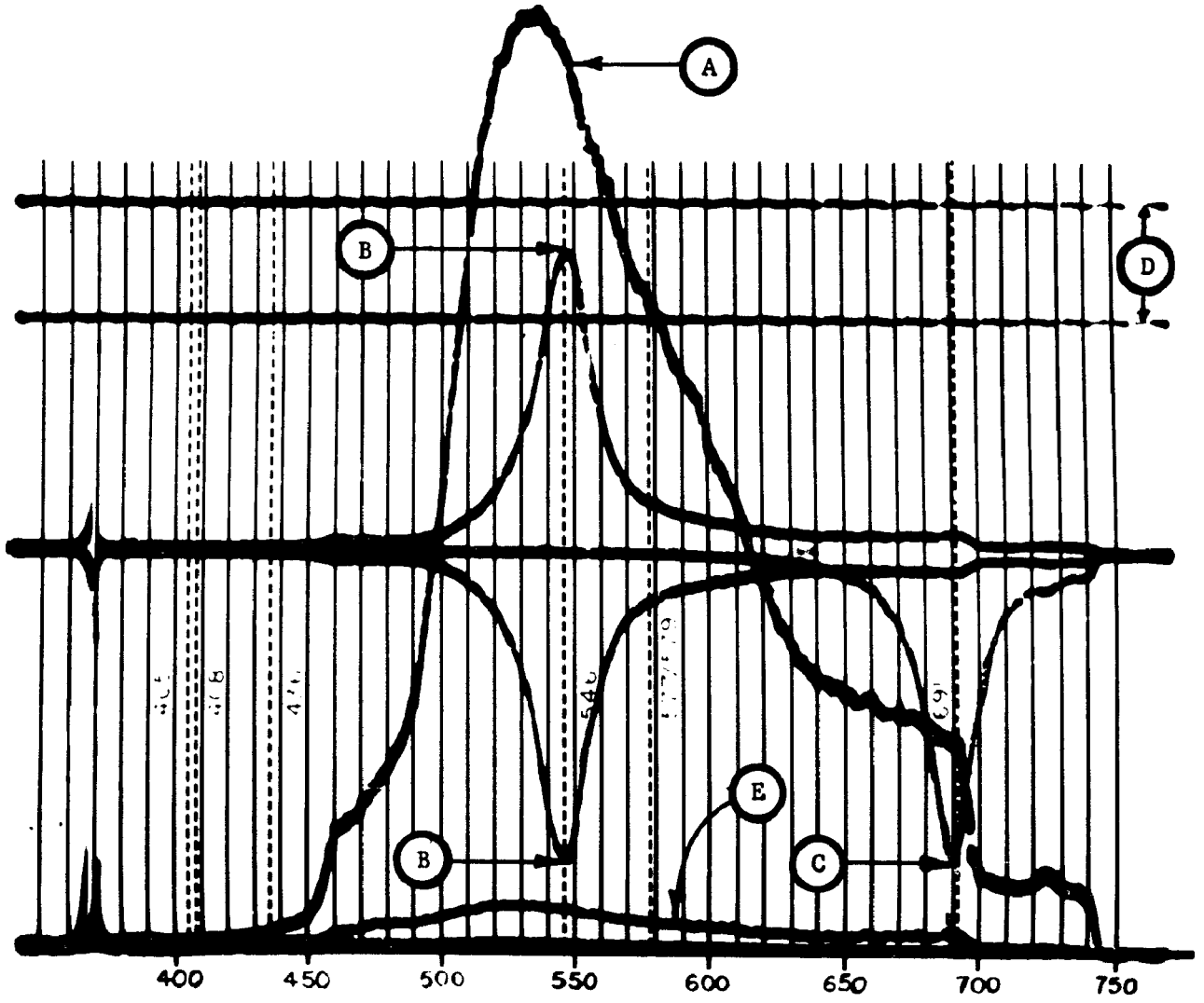
A
B
D
E
B
C
400
450
500
550
600
650
700
750

slide. If a photograph of the fluorescing cell were desired, it was taken immediately after recording the spectrum.

Fluorescence Fading

Cytoplasmic Granules in situ. Slides were prepared from the cell staining suspensions, AO per cell ratios ranging from 1.5×10^{-14} to 1.0×10^{-13} mole, and examined as previously described for fluorescence emission spectra. The variable photometric aperture was reduced to encompass a 6.8 μ^2 area within the cytoplasm of the cell. The image of the aperture superimposed on the image of the cell was photographed.

The MSF was switched to the fluorescence mode and the amplitude of fluorescence intensity at 660 nm was recorded as a function of time. The wavelength of fluorescence-excitation was 546 nm. Only one measurement was made per slide.

Isolated Cytoplasmic Granule. MCs were collected and stained in AO solutions as previously described. After the staining reaction reached equilibrium, the tube containing the staining suspension, 1.5×10^{-13} mole AO per cell, was placed in an ultrasonic cleaning bath (Model 8854-4, Cole-Parmer Inst. Co.) for approximately 1.5 min. Sonication disrupted the cell membrane causing a release of cytoplasmic granules. No effort was made to produce a granule suspension entirely free of intact cells. Granule preparations for fluorescence fading measurements were made by sealing a drop of the sonicate between a glass slide and coverslip as was

described for the intact cells. The experimental setup and technique for recording fading was the same as for granules *in situ*.

Electrophoretic Identification of the Acridine Orange - Acid Mucopolysaccharide Complex in MC Granules

MCs from three rats were isolated by centrifugation of the peritoneal washings layered over 35% albumin as previously described. After centrifugation, the MC fraction was washed twice in BPS to remove albumin.

A combination of the methods described by Lagunoff et al. (1964) and Uvnäs et al. (1970) was employed to disrupt the cell membrane and isolate the granules. MCs were suspended in 6.0 ml of deionized water and the pH adjusted to 7.1 with 0.1 M NaOH. The 15 ml round bottom test tube containing the suspension was alternately sonicated in the cleaning bath for 3 min and mixed (Super-Mixer, Lab-Line Inst. Inc.) vigorously for 1 min until approximately 90% of the cells were disrupted as determined by examination with a light microscope. The remaining intact cells and cell debris were removed by centrifugation at 200 X g for 7 min. The granule fraction remained in the supernatant which was collected and centrifuged at 1500 X g for 45 min to pellet the granules. All procedures were done at room temperature.

The granules were resuspended in 2.0 ml of deionized water and maintained at 65°C in a constant temperature bath until the granules were solubilized. Microscopic examination of samples taken

periodically from the suspension indicated the granules had dissolved after heating for 1 hour. To the solubilized granule solution, 0.5 ml of 0.5 M phosphate buffer (pH 8.0) and 4.6 mg pronase (Sigma Chemical Co., St. Louis, Missouri) were added and the mixture was incubated at 50°C for 24 hours for the digestion of granule protein.

The sample volume was made up to 4.0 ml with 0.01 M NaCl and applied to a column (1 X 25 cm) of 100-200 mesh Biogel P4 (Bio-Rad Laboratories, Richmond, California). It was eluted with 0.01 M NaCl; the first 6.0 ml, void volume, were discarded and the next 9.0 ml fraction containing acid mucopolysaccharides (AMPS) was collected. The eluate was lyophilized and 25.0 ml of deionized water were added to the residue.

The electrophoretic identification of the AMPS present in the chromatographic fraction on cellulose acetate was done essentially by the procedure described by Herd (1968). Savant flat plate electrophoresis apparatus with circulating bath at 2°C was used for separation. Electrophoresis was run at pH 3.0 in pyridine/formic acid buffer for 1.5 to 2.0 hours at 100 volts per strip. The strips were stained for 2 min in 1% alcian blue in 5% acetic acid and then rinsed in a 5% acetic acid bath.

The reference standards were generously provided by Dr. J. A. Cifonelli and Dr. M. B. Mathews of the University of Chicago and Dr. L. Rodén of the University of Alabama in Birmingham.

RESULTS

Equilibrium Binding

The fluorometer was used to measure the intensity of fluorescence of the serial dye dilutions used for staining cells. Fluorescence intensity was measured at 540 nm, the emission maximum of the AO monomer band. A 2 mm pathlength cuvette was used for all measurements. Figure 6 shows a typical fluorescence intensity versus AO concentration curve over a range of 2.75×10^{-7} to 4×10^{-5} M. The fluorescence intensity was a linear function (slope = 1.0) of AO concentration up to approximately 8×10^{-6} M. At higher concentrations, the rate of change in fluorescence intensity decreased over the range of concentrations used in this study.

The nonlinear behavior at concentrations higher than 8×10^{-6} M was the result of exciting and emitted light absorption by the solution and also self-aggregation of the dye which decreased the concentration of the monomeric species with a concomitant quenching of the emission at 540 nm. In comparing the relative intensity of fluorescence versus AO concentration using 2 mm and 10 mm pathlength cuvettes, the 2 mm cuvette was chosen because the measured intensity was linear over a wider range of concentration. In the 10 mm pathlength cuvette, more of the exciting light was absorbed before reaching the volume of solution giving rise to the measured

FIGURE 6

Fluorescence intensity measured at 540 nm of cell staining solutions as a function of AO concentration. Cuvette pathlength = 2 mm.

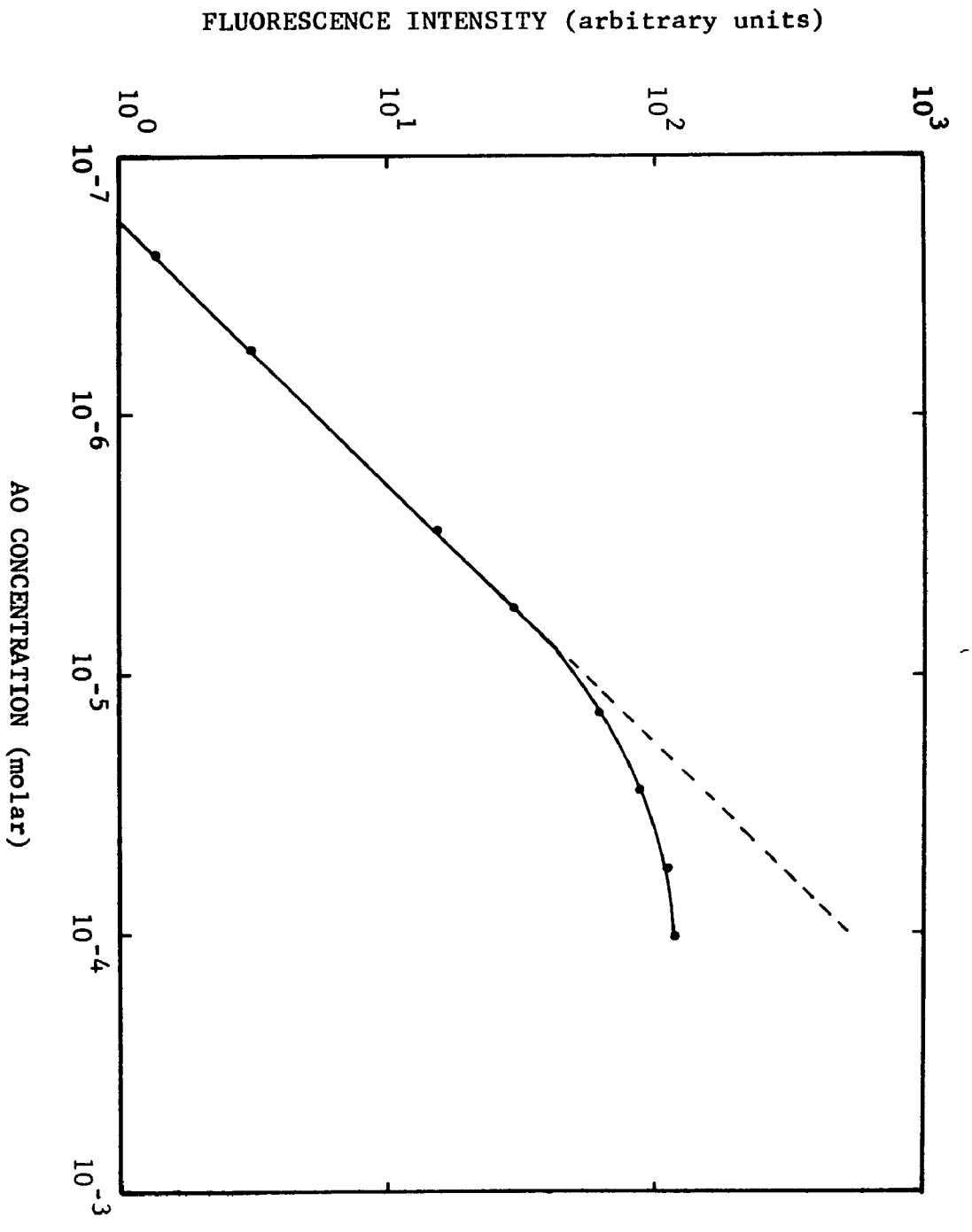
FLUORESCENCE INTENSITY (arbitrary units)
10^0
10^1
10^2
10^3
AO CONCENTRATION (molar)
10^{-7}
10^{-6}
10^{-5}
10^{-4}
10^{-3}

fluorescence; this was particularly noticeable for dye concentrations greater than approximately 3×10^{-6} M.

Fluorescence intensity measurements of the dye in the staining tube supernatants and control tubes were used to determine the average intracellular dye content at equilibrium. The amount of dye sequestered by the cells was the difference in the amount of dye initially presented to the cells and that remaining in solution and that bound to the glass tube. The slight binding of AO by glass in the staining tube and control tube was approximately the same, and any difference was negligible compared with the amount of AO removed from solution by the cells. The amount of free dye, expressed in moles per cell at equilibrium, was calculated by multiplying the quantity of AO initially available to the cells by the ratio of the supernatant to control fluorescence intensities and dividing that quantity by the total number of cells in the staining suspension.

Figure 7 is a log log plot of the average amount of dye taken up per cell as a function of free dye per cell remaining in the supernatant at equilibrium. No portion of the curve which extends over approximately 3 decades is perfectly linear. However, from an average dye uptake per cell of about 3.0×10^{-17} to 1.5×10^{-15} mole, the curve can be approximated with a straight line having a slope of 2.0. The slope gradually decreases as the cells take up more and more dye. Saturation appears to occur with an intracellular dye content of approximately 1.4×10^{-13} mole per cell.

A Scatchard plot of binding data is shown in Figure 8 which consists of a plot of dye uptake per cell in moles divided by the

FIGURE 7

Average AO uptake by mast cells as a function of equilibrium free dye available per cell.

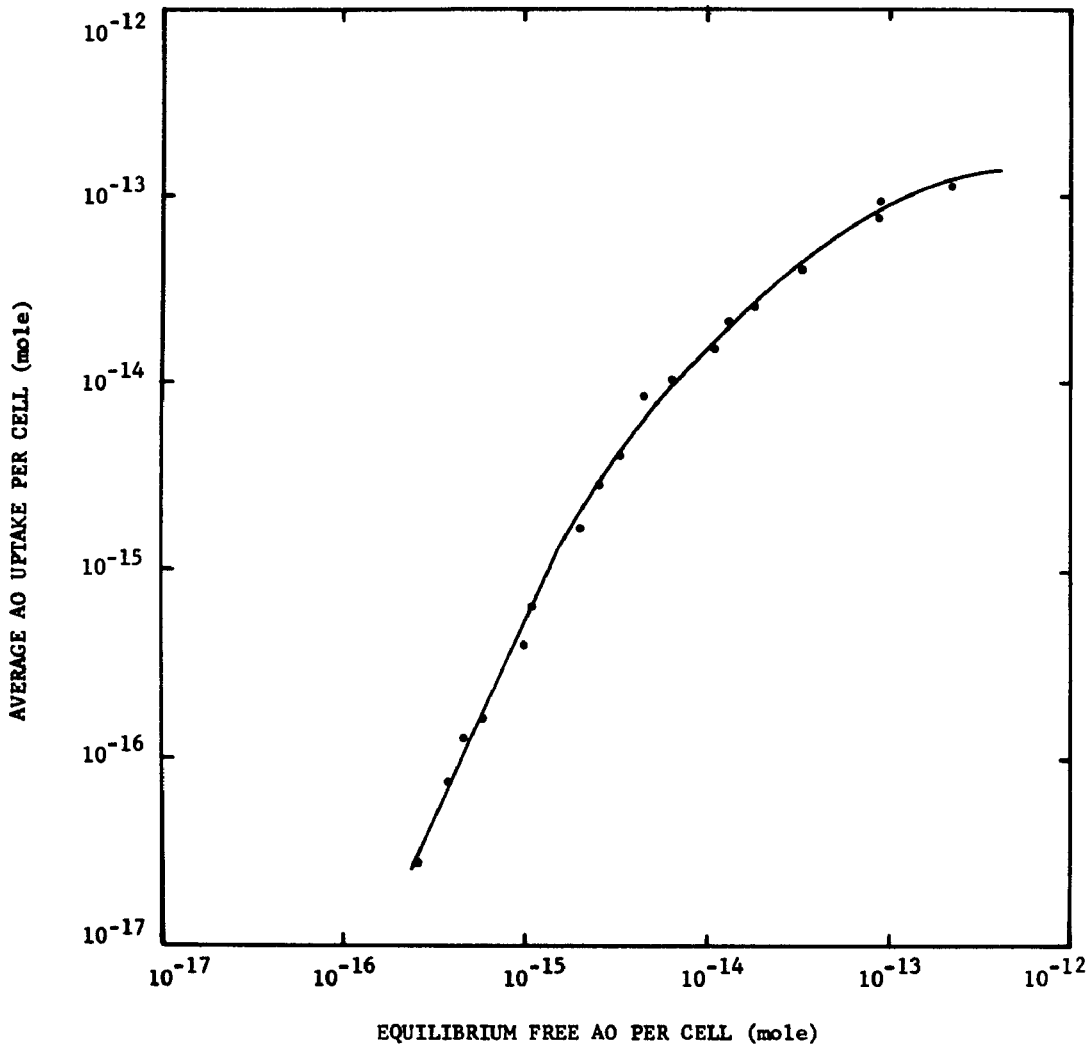
AVERAGE AO UPTAKE PER CELL (mole)
10^-12
10^-13
10^-14
10^-15
10^-16
10^-17
10^-17
10^-16
10^-15
10^-14
10^-13
10^-12
EQUILIBRIUM FREE AO PER CELL (mole)

FIGURE 8

Scatchard plot of AO-mast cell binding data.

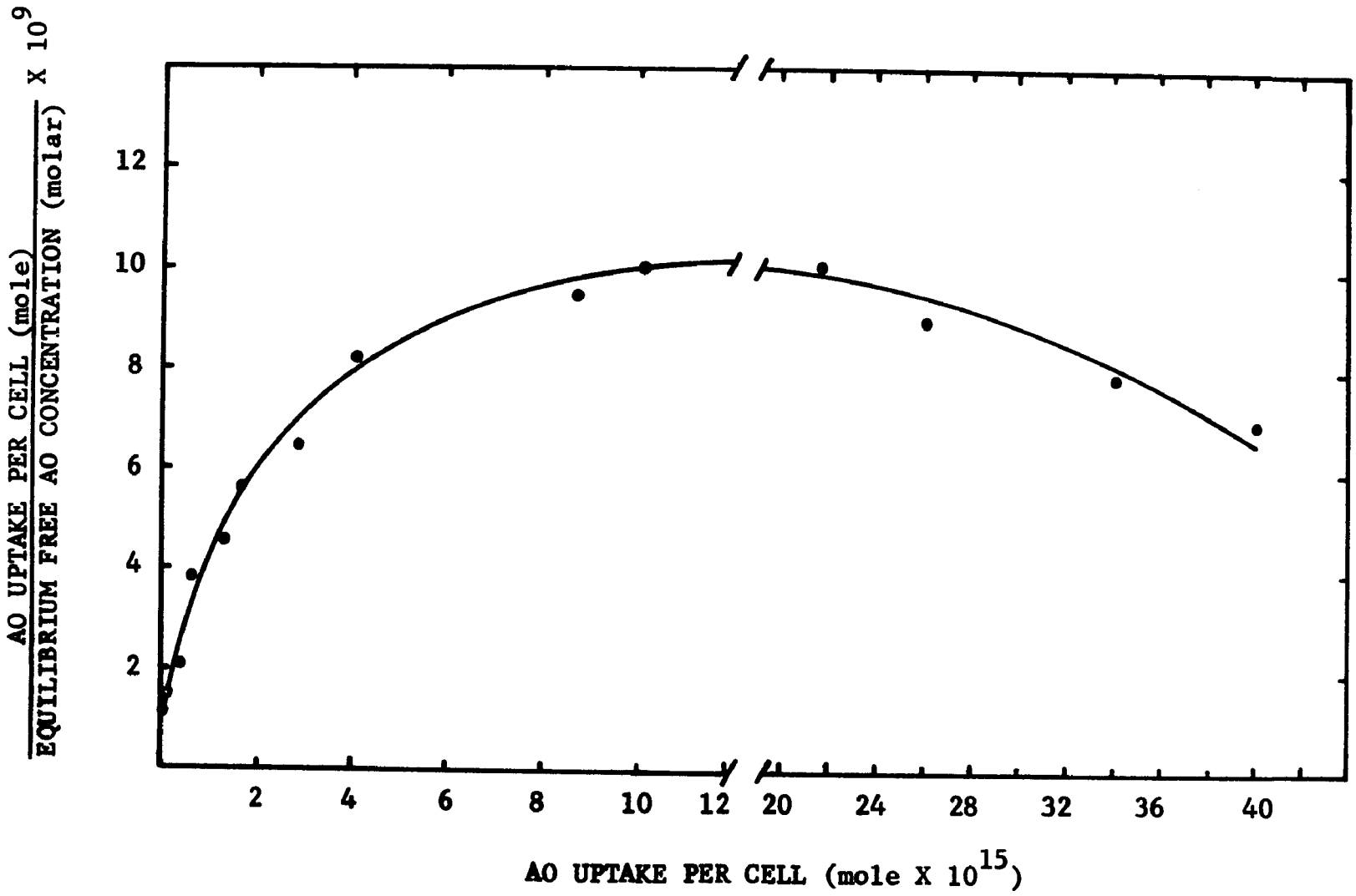
AO UPTAKE PER CELL (mole) / EQUILIBRIUM FREE AO CONCENTRATION (molar) X 10^9
12
10
8
6
4
2
2
4
6
8
10
12
20
24
28
32
36
40
AO UPTAKE PER CELL (mole X 10^15)

molar concentration of the free dye at equilibrium versus the dye uptake per cell.

Visual Observations

Figure 9 is a photomicrograph of a typical population of MCs that were separated from other peritoneal cells by the centrifugation technique using 35% albumin.

MCs within a given staining population exhibited variations in color of fluorescence. However, certain staining features were common to cells containing the same average amount of dye. Cells containing small quantities of dye, less than approximately 2×10^{-16} mole AO per cell, exhibited extremely dim green fluorescence and were not bright enough to adequately expose the type of photographic film (High Speed Ektachrome, Eastman Kodak) used. No morphological features were distinguishable at these low dye concentrations. As the intracellular dye concentration was increased, the intensity of fluorescence increased and certain morphological features became apparent (Figures 10-15).

Figure 10 is representative of the variation in fluorescence of cells from a staining population with an average intracellular dye content of 2.3×10^{-16} mole AO, the range in which cells exhibited only green fluorescence. A structure thought to be the nucleolus or perhaps condensed chromatin was clearly defined in each of the cells and appeared brighter than other nuclear constituents which did not stain in all cells. The nonstaining nucleus

FIGURE 9

Photomicrograph of mast cell preparation under a Smith interference microscope with tungsten light source without a filter.

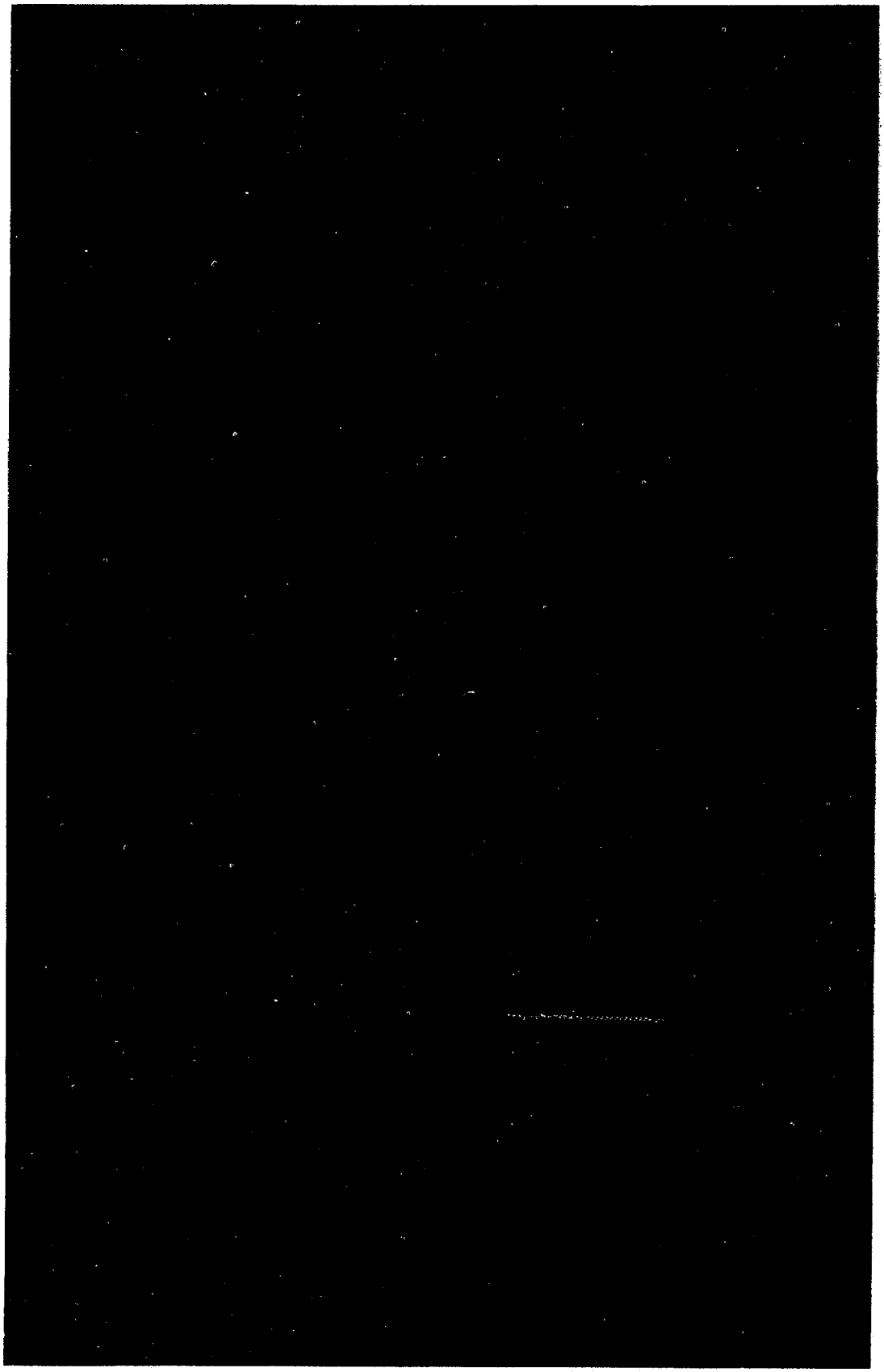

with the exception of the nucleolus appeared as a dark hole within the fluorescence image of the cell (Figure 10a). Alternatively, nuclear fluorescence in some cells, with the exception of the nucleolus, was generally uniform throughout the nucleus (Figure 10b). The cytoplasmic fluorescence of cells which had nuclear fluorescence was fainter and more diffuse than observed in cells with an absence of nuclear fluorescence. Occasional green cytoplasmic granules were often seen in cells without nuclear fluorescence.

As the quantity of intracellular dye was increased, nuclear fluorescence became brighter and changed from green to yellow. The nucleus appeared green-yellow at approximately 1×10^{-14} mole AO per cell and was completely yellow at intracellular dye contents higher than 5×10^{-14} mole. Cells containing more than approximately 5×10^{-14} mole AO exhibited either red fluorescence throughtout the entire cell or a yellow-orange nucleus and red cytoplasmic granules (Figures 14 and 15). Since the nucleus in some cells was completely surrounded by cytoplasmic granules, it was not always possible to determine the true color of the nuclear fluorescence in cells containing large amounts of dye.

Metachromatic staining was observed in cytoplasmic granules of cells with an average dye uptake as low as approximately 5×10^{-16} mole. Staining did not occur uniformly in all granules, some granules within a given cell fluoresced green and others red (Figure 11). Most granules fluoresced red with intracellular dye quantities greater than approximately 1×10^{-14} mole which is about

FIGURE 10

Photomicrographs of fluorescing cells containing an average of 2.27×10^{-16} mole AO.

FIGURE 11

Photomicrographs of fluorescing cells containing an average of 2.10×10^{-15} mole AO.

FIGURE 12

Photomicrographs of fluorescing cells containing an average of 4.69×10^{-15} mole AO.

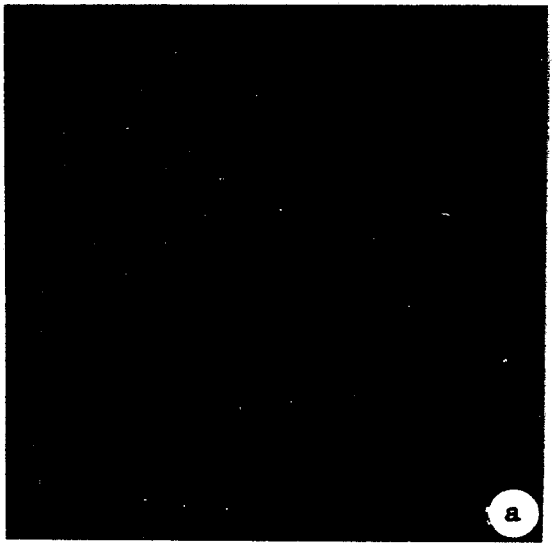
a

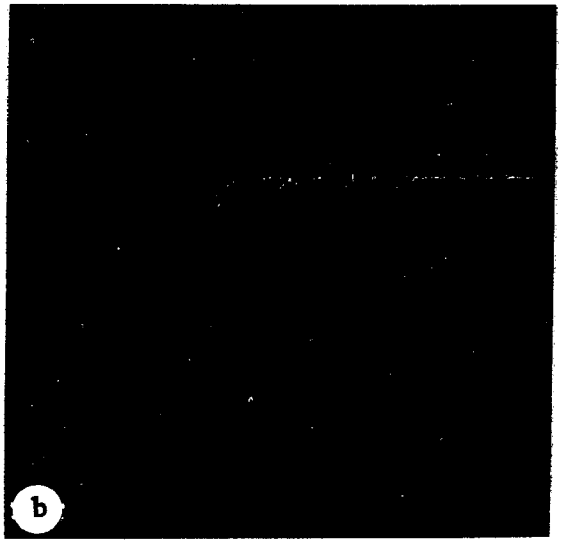
b

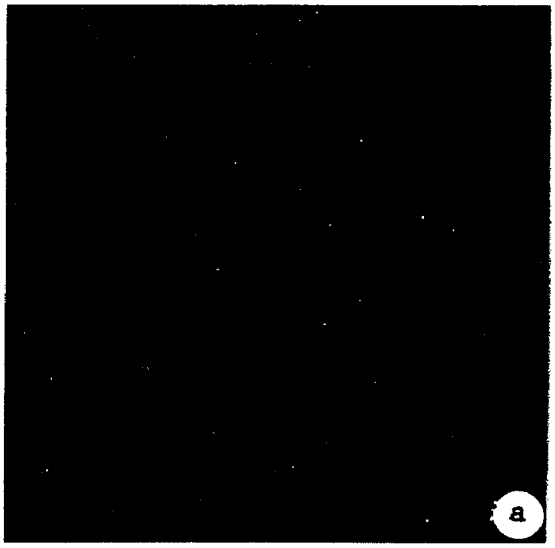
a

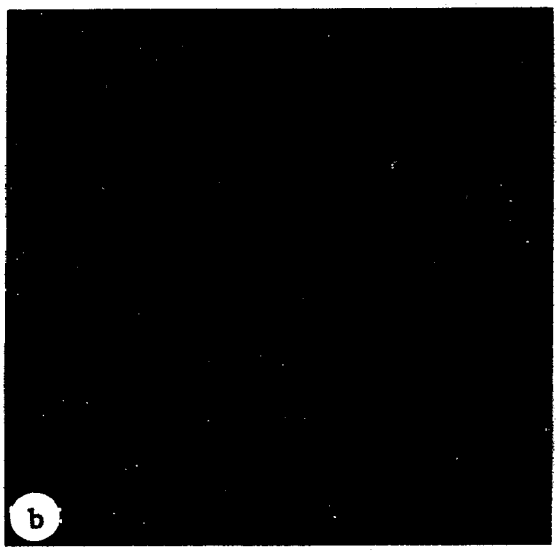
b

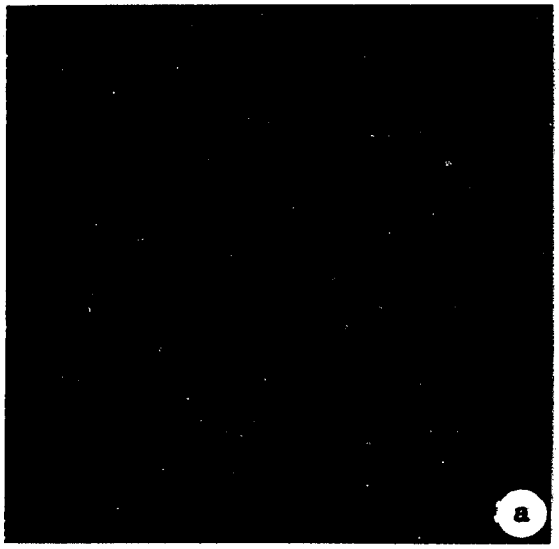
a

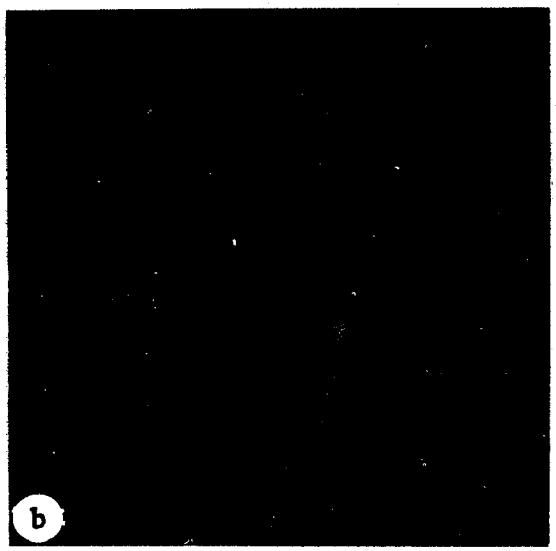
b

FIGURE 13

Photomicrographs of fluorescing cells containing an average of 2.48×10^{-14} mole AO.

FIGURE 14

Photomicrographs of fluorescing cells containing an average of 5.89×10^{-14} mole AO.

FIGURE 15

Photomicrographs of fluorescing cells containing an average of 1.30×10^{-13} mole AO.

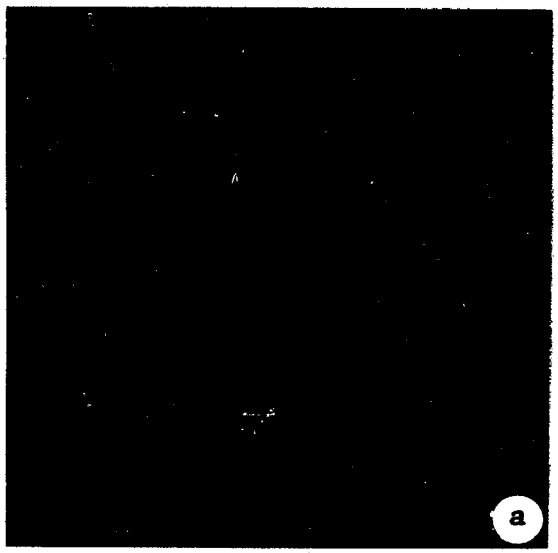
a

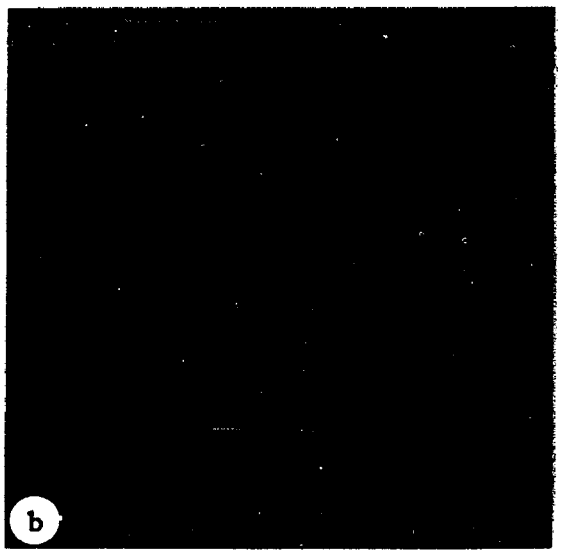
b

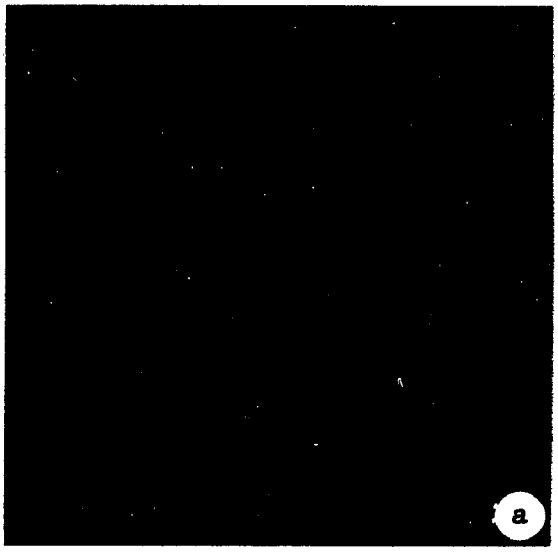
a

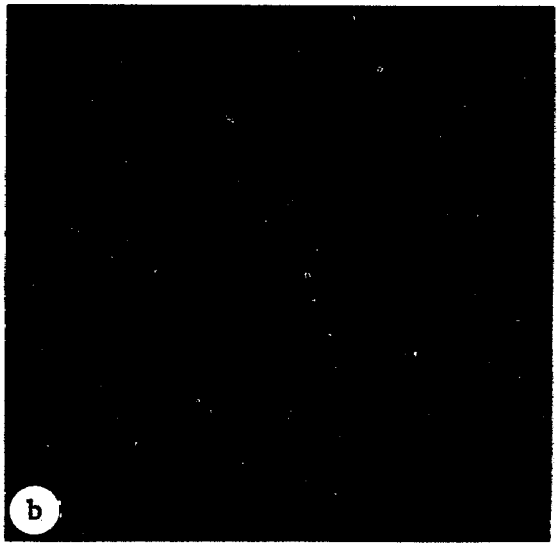
b

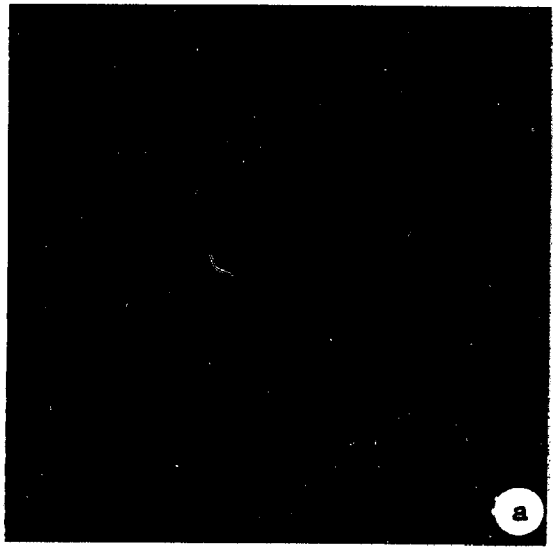
a

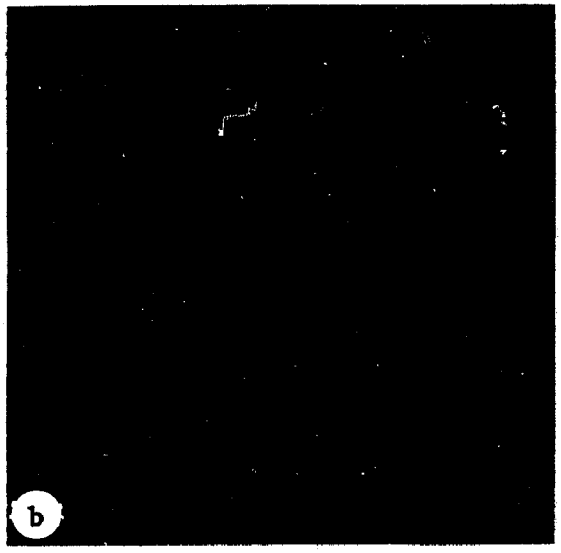
b

one-half decade lower than is required to produce orange staining nuclei.

Fluorescence Measurements

Fluorescence Emission Spectra from Single Cells

Corrected fluorescence emission spectra normalized with respect to maximum fluorescence intensity and with fluorescence intensity given in terms of ppu are shown in Figures 16-19. In the remainder of this paper, normalized spectra will be used to refer to spectra normalized with respect to maximum fluorescence intensity.

Figure 16 shows changes in the emission spectra as a function of intracellular dye content. At the lowest dye concentration, 1.65×10^{-16} mole per cell (cell 4622), a single emission maximum occurred at approximately 530 nm. Shoulders at 600 and 670 nm indicated the possible presence of more than one spectroscopic species in this region of the spectrum. Variability in fluorescence intensity existed among cells at this low staining concentration. However, the spectral shapes were the same with a half-value bandwidth of 90 nm which corresponds to 5.5×10^{3} cm^{-1}.

As the dye content of the cell was increased, the slight shoulder at 600 nm disappeared and the amplitude of fluorescence at 670 nm increased relative to the 535 nm peak until finally a single emission maximum emerged at 670 nm. Fluorescence emission at 535 nm appeared as a slight shoulder in the spectra of cells containing 1×10^{-14} to 4×10^{-14} mole of dye. The green fluorescing species

FIGURE 16

Normalized corrected fluorescence emission spectra of individual mast cells.

Cell No.	Intracellular AO (mole)
4622	1.65×10^{-16}
4623	5.40×10^{-16}
4631	3.35×10^{-15}
4639	2.00×10^{-14}
4502	3.60×10^{-14}
4507	1.34×10^{-13}

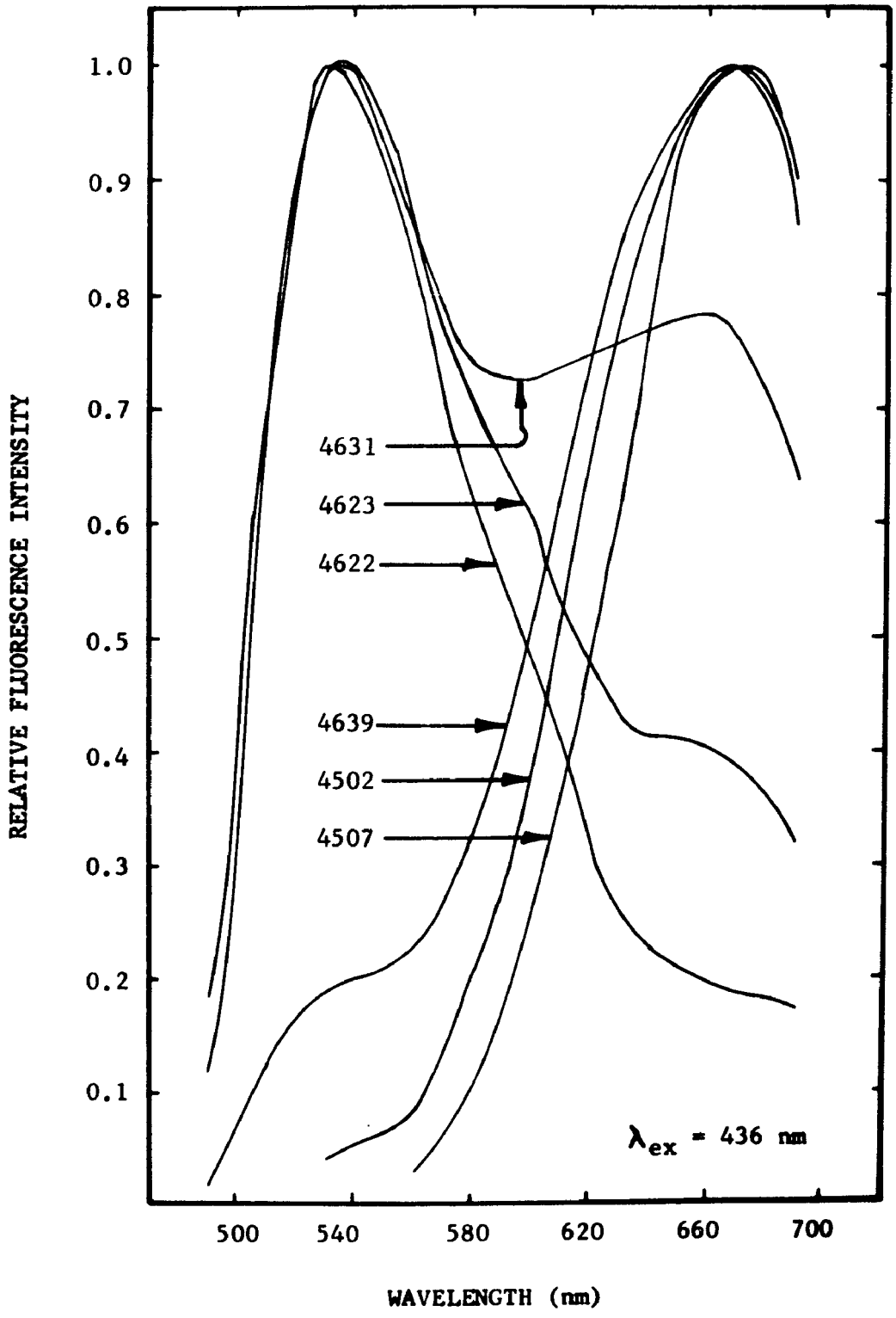
RELATIVE FLUORESCENCE INTENSITY
1.0
0.9
0.8
0.7
0.6
0.5
0.4
0.3
0.2
0.1
4631
4623
4622
4639
4502
4507
λex = 436 nm
500
540
580
620
660
700
WAVELENGTH (nm)

FIGURE 17

Corrected fluorescence emission spectra of individual mast cells. Experimental data of Figure 16 plotted in terms of ppu.

Cell No.	Intracellular AO (moles)
4622	1.65×10^{-16}
4623	5.40×10^{-16}
4631	3.35×10^{-15}
4639	2.00×10^{-14}
4502	3.60×10^{-14}
4507	1.34×10^{-13}

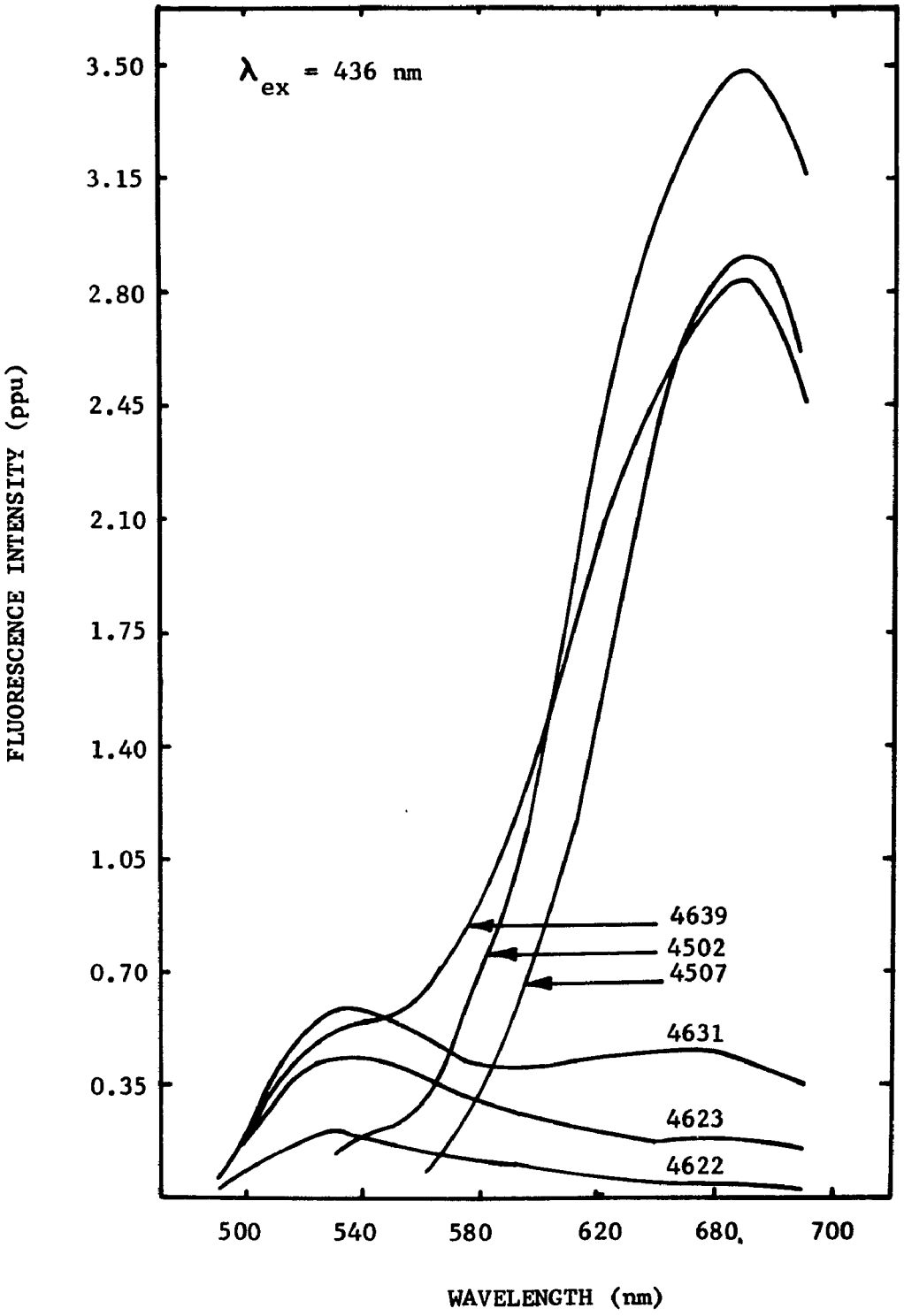
λ_{ex} = 436 nm
3.50
3.15
2.80
2.45
2.10
1.75
1.40
1.05
0.70
0.35
FLUORESCENCE INTENSITY (ppu)
4639
4502
4507
4631
4623
4622
500
540
580
620
680
700
WAVELENGTH (nm)

FIGURE 18

Normalized corrected fluorescence emission spectra of individual mast cells containing an average of 3.35×10^{-15} mole AO.

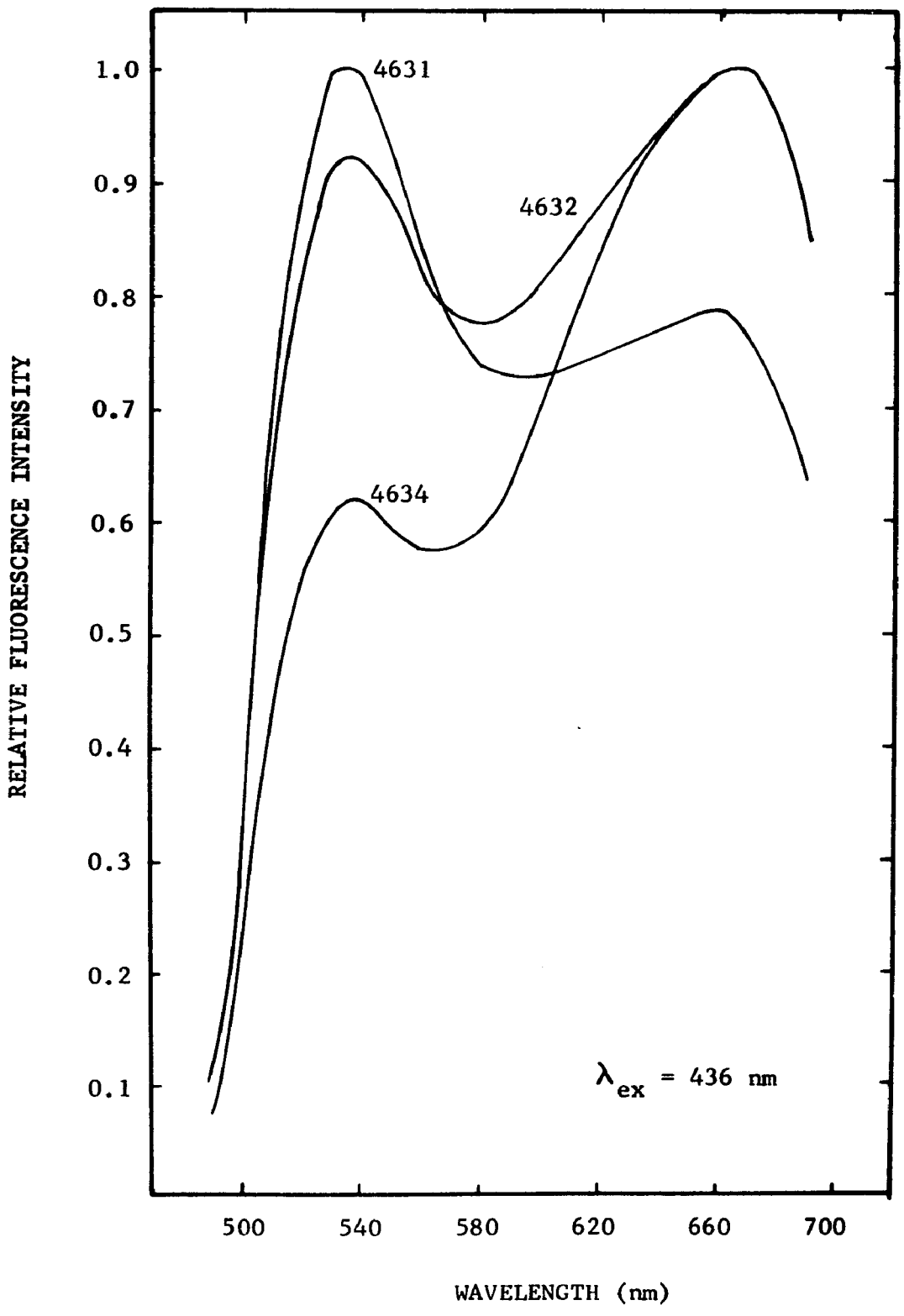
RELATIVE FLUORESCENCE INTENSITY
1.0
0.9
0.8
0.7
0.6
0.5
0.4
0.3
0.2
0.1
4631
4632
4634
λ_{ex} = 436 nm
500
540
580
620
660
700
WAVELENGTH (nm)

FIGURE 19

Corrected fluorescence emission spectra of individual mast cells containing an average of 3.35×10^{-15} mole AO. Experimental data of Figure 18 plotted in terms of ppu.

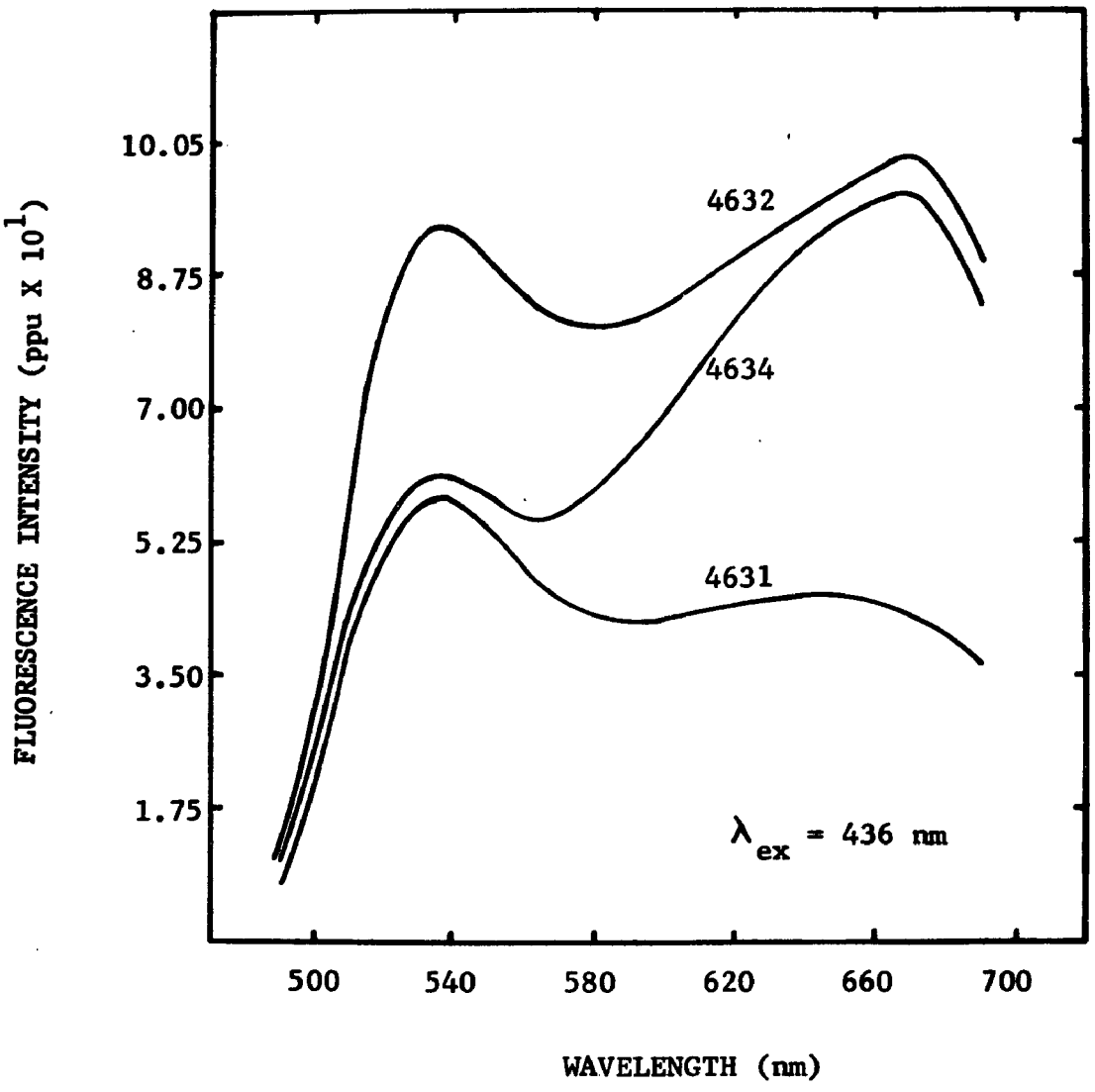
FLUORESCENCE INTENSITY (ppu x 10^1)
10.05
8.75
7.00
5.25
3.50
1.75
4632
4634
4631
λ_{ex} = 436 nm
500
540
580
620
660
700
WAVELENGTH (nm)

were not observed in the spectra of cells having an intracellular dye content greater than approximately 6 X 10^{-14} mole.

Variation in spectral shape was negligible among cells within staining populations having a very low or a very high average dye content. Although spectra exhibited two distinct maxima within the mid-range (1 X 10^{-15} to 1 X 10^{-14} mole AO per cell) of concentrations studied, spectral variability was apparent. Figure 18 shows the normalized corrected spectra of three cells having an average dye content of 3.35 X 10^{-15} mole. The fluorescence intensity of cell 4631 was greater at 535 nm than at 670 nm. Conversely, the amplitude of the 670 nm peak was greater for cells 4632 and 4634. The spectra of the latter cells also exhibited different relative intensities of emission at 535 nm.

Corrected emission spectra with fluorescence intensity given in terms of ppu are shown in Figures 17 and 19 demonstrating changes in fluorescence intensity as a function of intracellular dye which are not reflected in the corresponding normalized plots of the data (Figures 16 and 18).

The intensity of fluorescence emission at 535 nm and 670 nm as a function of average dye uptake per cell, ranging from approximately 1.2 X 10^{-16} to 1.5 X 10^{-13} mole, is shown in Figure 20. Each point on the curve represents the average fluorescence intensity measurement of three to five cells taken from the same staining population.

Fluorescence emission at 535 nm increased with a decreasing rate as more dye was complexed with the cell up to approximately

FIGURE 20

Fluorescence intensity at 535 nm and 670 nm of individual mast cells as a function of intracellular dye content.

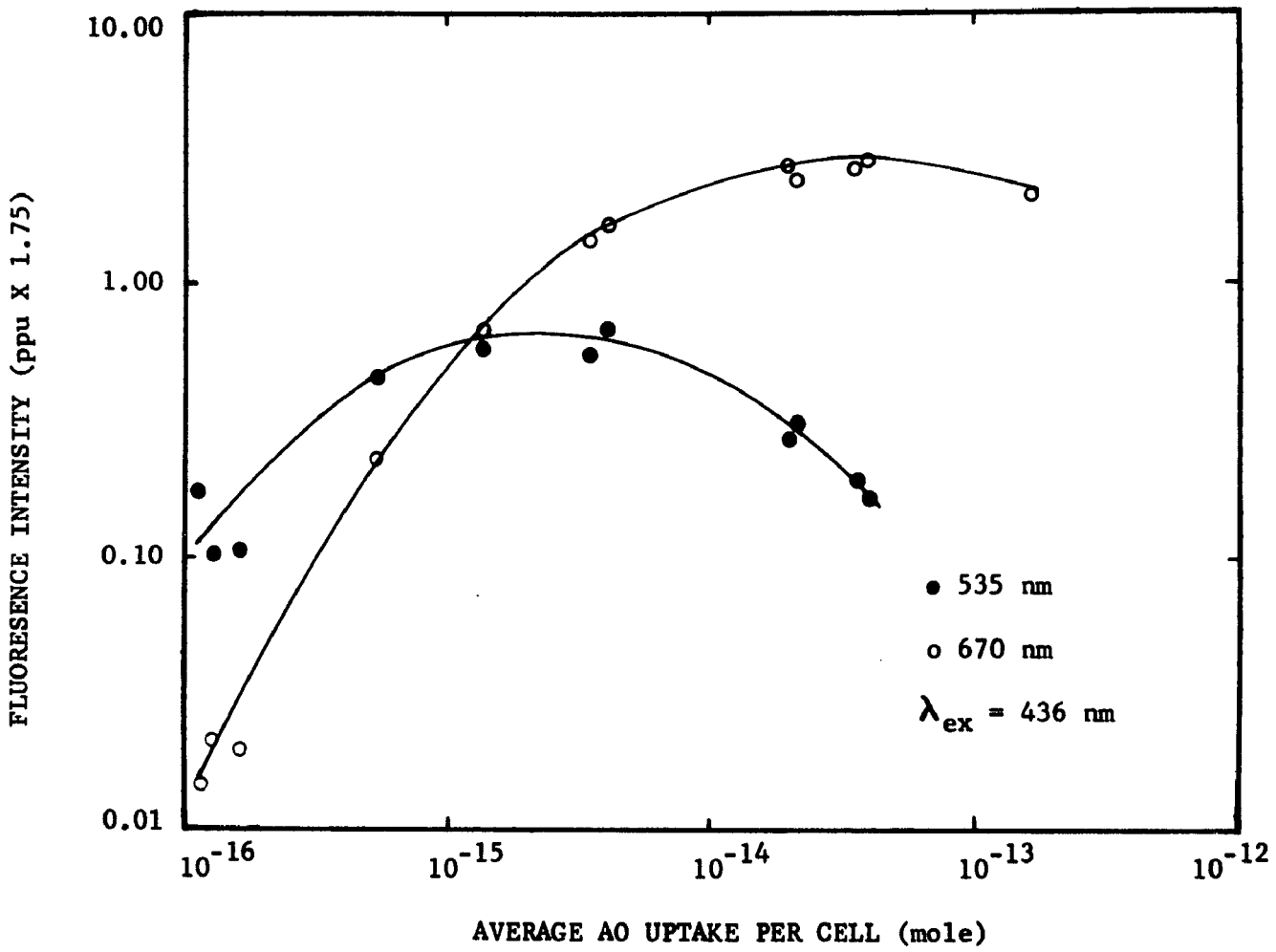
10.00
1.00
0.10
0.01
FLUORESENCE INTENSITY (ppu X 1.75)
10^-16
10^-15
10^-14
10^-13
10^-12
AVERAGE AO UPTAKE PER CELL (mole)
● 535 nm
o 670 nm
λex = 436 nm

3.5×10^{-15} mole. At higher concentrations, a gradual decrease in fluorescence intensity at 535 nm was observed. This emission band was absent in cells containing more than 4×10^{-14} mole AO. A 535 nm fluorescence emission maximum was observed in spectra of cells containing less than approximately 1.5×10^{-15} mole AO. Cells containing more dye demonstrated a 670 nm emission maximum, the intensity of which was greatest at approximately 4×10^{-14} mole AO per cell. Figure 20 shows that the intensity of red emission, like that of green fluorescence, does not vary linearly with intracellular dye content but increases with a decreasing rate up to a maximum and then decreases with increasing amounts of dye.

Figure 21 shows the log of the ratio of fluorescence intensity at 670 nm to that at 535 nm versus the log of AO uptake per cell. This log log plot is a straight line with a slope of 0.77 over the range of AO uptake per cell in which both spectroscopic species were present.

Fluorescence Fading Measurements

Intact Cells. Fading of fluorescence of stained cells occurred slowly enough so that it was possible to measure the fading phenomenon by recording a series of emission spectra at appropriate time intervals after initial excitation. Figures 22-24 are representative of changes observed in fluorescence emission spectra of MCs as a function of irradiation time and demonstrate differences resulting over a range of intracellular dye quantities.

FIGURE 21

Ratio of fluorescence intensities, 670 nm: 535 nm, from individual mast cells as a function of intracellular dye.

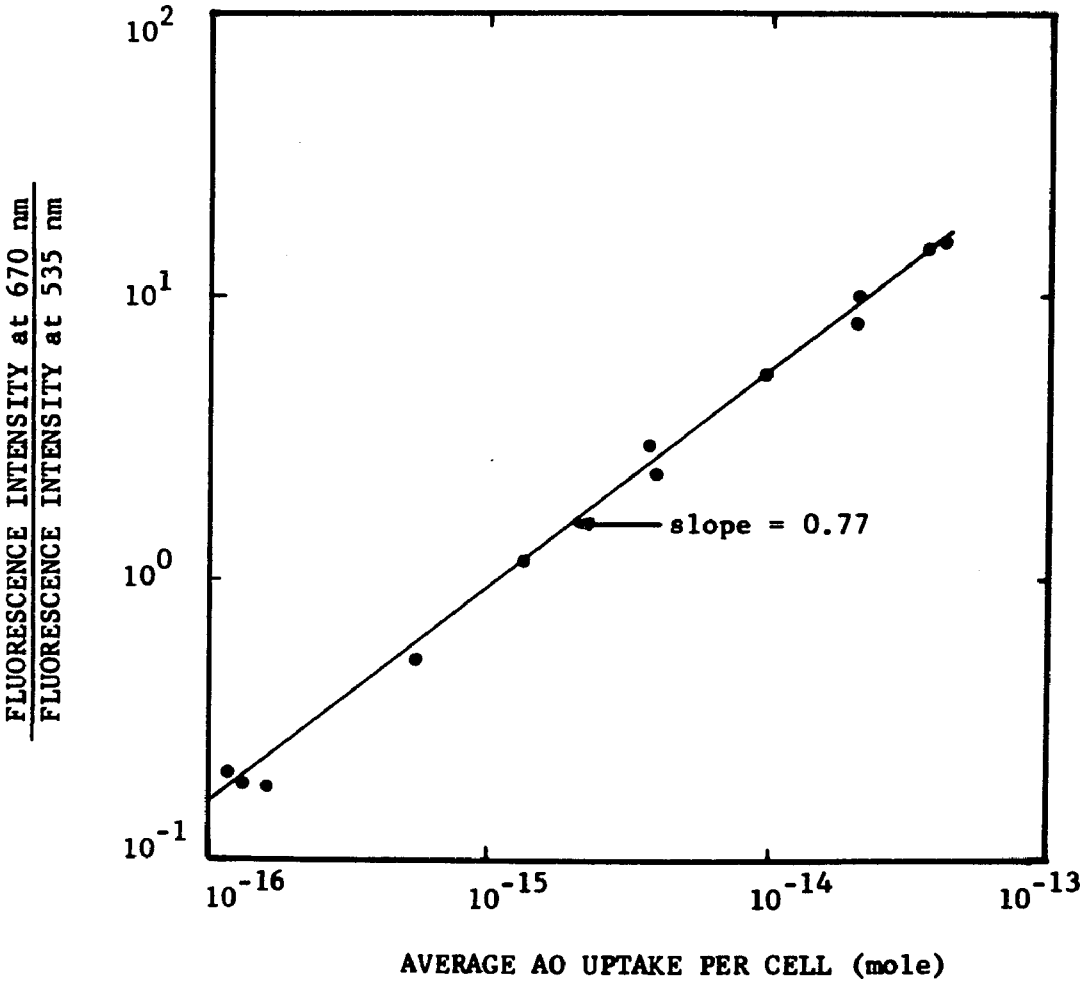
10^2
10^1
10^0
10^{-1}
FLUORESCENCE INTENSITY at 670 nm / FLUORESCENCE INTENSITY at 535 nm
slope = 0.77
10^{-16}
10^{-15}
10^{-14}
10^{-13}
AVERAGE AO UPTAKE PER CELL (mole)

FIGURE 22

Corrected fluorescence emission spectra of a continuously irradiated mast cell containing an average of 1.16×10^{-16} mole AO. λ_{ex} = 436 nm.

Spectrum	Irradiation Time (seconds)
A	0
B	36
C	65

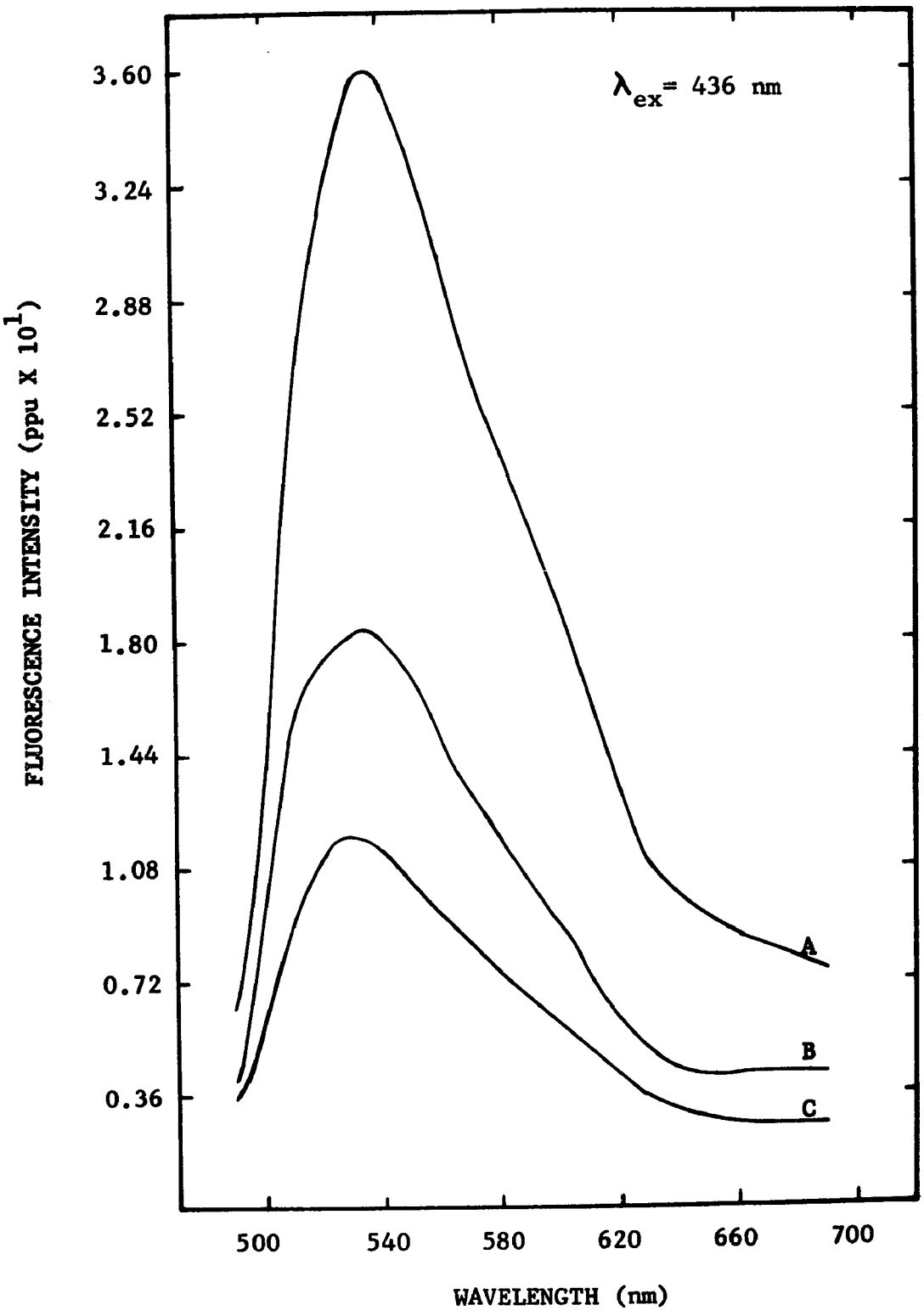
λ_{ex}= 436 nm
3.60
3.24
2.88
2.52
2.16
1.80
1.44
1.08
0.72
0.36
FLUORESCENCE INTENSITY (ppu X 10^1)
A
B
C
500
540
580
620
660
700
WAVELENGTH (nm)

FIGURE 23

Corrected fluorescence emission spectra of a continuously irradiated mast cell containing an average of 1.16×10^{-14} mole AO. λ_{ex} = 436 nm.

Spectrum	Irradiation Time (seconds)
A	0
B	12
C	40
D	62
E	135
F	360

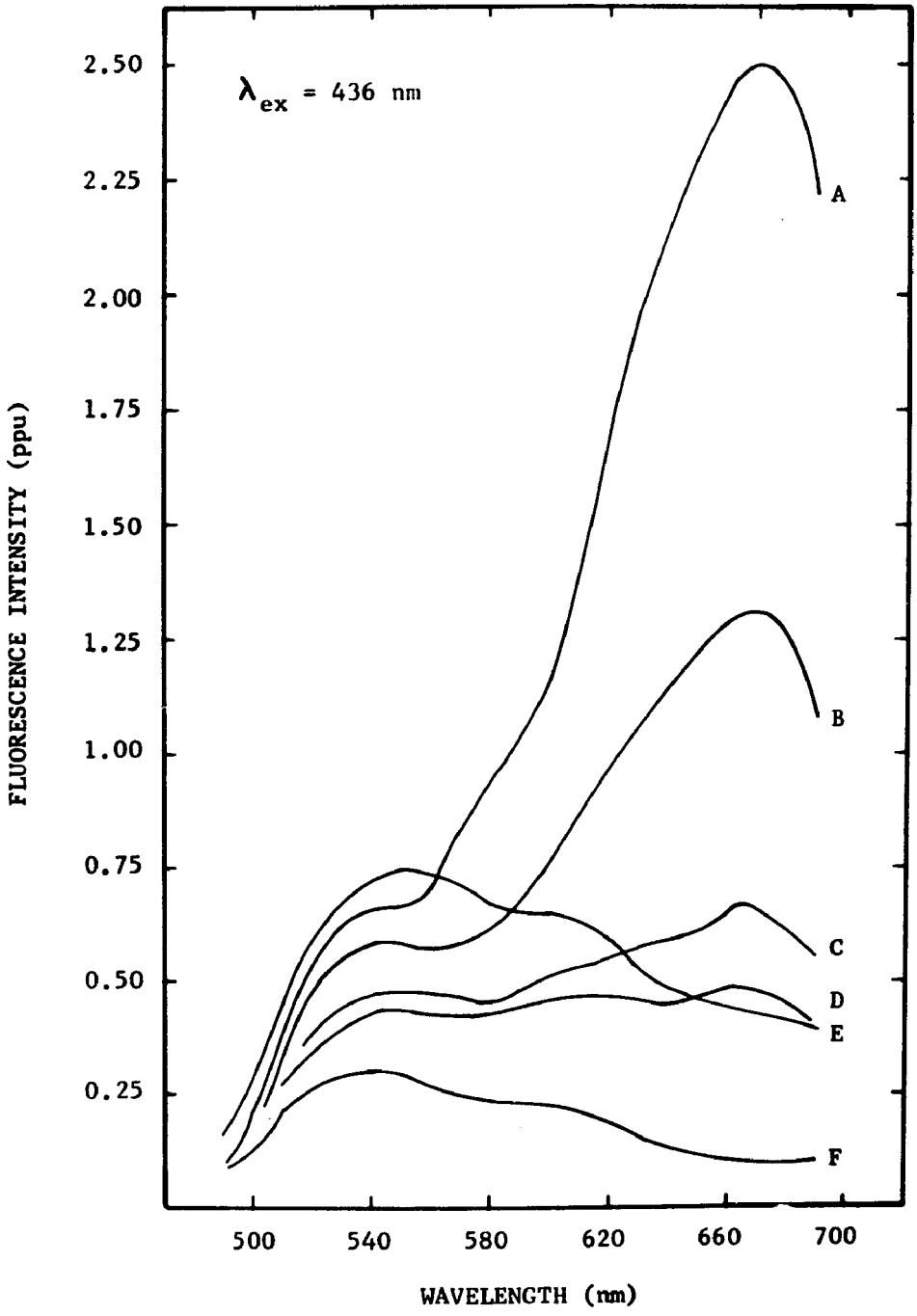
λ_{ex} = 436 nm
2.50
2.25
2.00
1.75
1.50
1.25
1.00
0.75
0.50
0.25
FLUORESCENCE INTENSITY (ppu)
500
540
580
620
660
700
WAVELENGTH (nm)
A
B
C
D
E
F

FIGURE 24

Corrected fluorescence emission spectra of a continuously irradiated mast cell containing an average of 1.10×10^{-13} mole AO. λ_{ex} = 436 nm.

Spectrum	Irradiation Time (seconds)
A	0
B	13
C	68

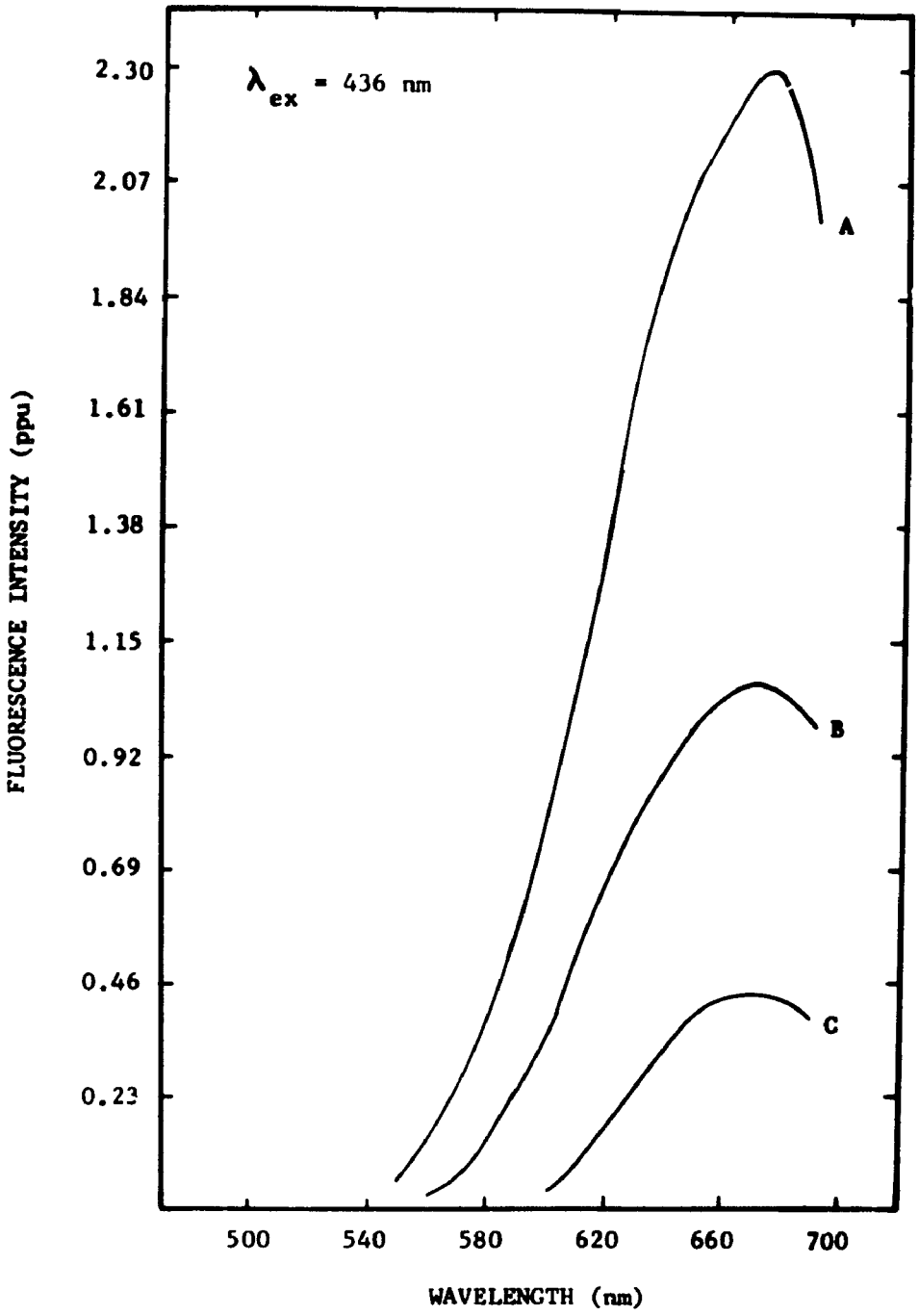
λ_{ex} = 436 nm
2.30
2.07
1.84
1.61
1.38
1.15
0.92
0.69
0.46
0.23
FLUORESCENCE INTENSITY (ppu)
A
B
C
500
540
580
620
660
700
WAVELENGTH (nm)

Figures 25 and 26 demonstrate the changes in the intensity of fluorescence emission at 535 and 670 nm resulting from continuous excitation. The fluorescence fading curves were derived from a series of emission spectra similar to those shown in Figures 22-24. The emission spectra were obtained under the same experimental conditions (I_{ex}, optical set-up, etc.) because both intensity of fluorescence and fading rate are a function of I_{ex} (Golden and West, 1974).

Figure 25 shows the fluorescence fading behavior, 670 nm of cells containing quantities of AO ranging from 1.35×10^{-15} to 1.38×10^{-13} mole. Each curve exhibits a large initial decrease in intensity followed by a more gradual decrease. The rate of fading generally increased with increasing amounts of intracellular dye. An increase in emission of the red fluorescing species was never observed with continuous excitation.

The molecular species responsible for emission at 535 nm demonstrated fading behavior markedly different from that of the red-fluorescing species. An initial decrease in green fluorescence was observed in all cells. Cells containing more than approximately 1×10^{-14} mole AO had fading characteristics less predictable than those cells containing smaller quantities of dye.

Two features common to the fluorescence fading behavior measured at 535 nm of cells containing more than 1×10^{-14} mole AO are: an initial decrease in intensity occurred, and the intensity after approximately 2 min exposure to fluorescence-excitation was less than the initial value. Figure 26 shows the intensity of

FIGURE 25

Fluorescence intensity changes at 670 nm of individual mast cells continuously irradiated. λ_{ex} = 436 nm.

Cell No.	Intracellular AO (mole)
4342	1.35×10^{-15}
3521	1.37×10^{-14}
4314	2.41×10^{-14}
3881	1.38×10^{-13}

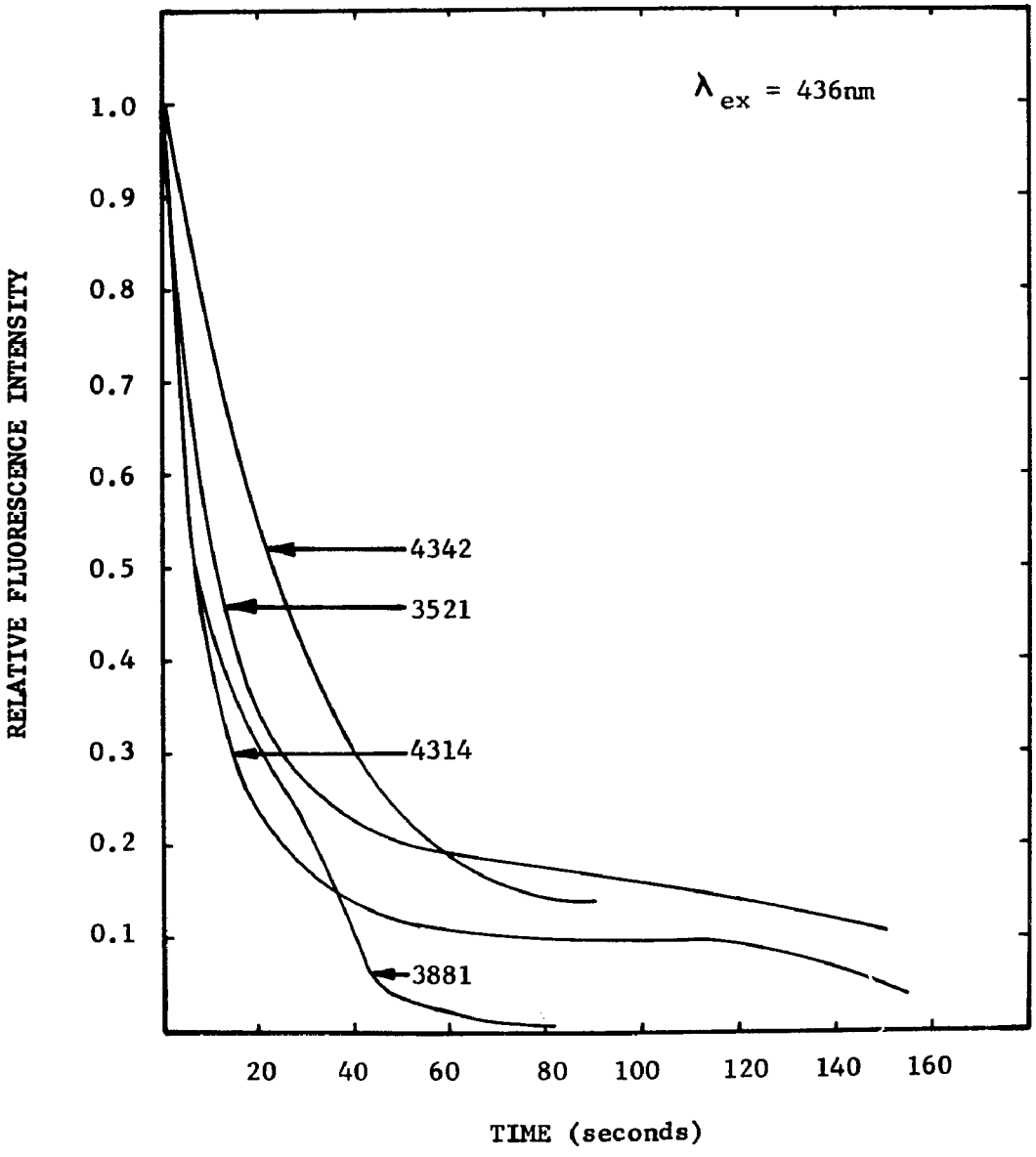
λ_{ex} = 436nm
RELATIVE FLUORESCENCE INTENSITY
1.0
0.9
0.8
0.7
0.6
0.5
0.4
0.3
0.2
0.1
4342
3521
4314
3881
20
40
60
80
100
120
140
160
TIME (seconds)

FIGURE 26

Fluorescence intensity changes at 535 nm of individual mast cells continuously irradiated. λ_{ex} = 436 nm.

Cell No.	Intracellular AO (mole)
4365	1.16×10^{-16}
3565	1.21×10^{-15}
3521	1.37×10^{-14}
4314	2.41×10^{-14}
4291	3.91×10^{-14}

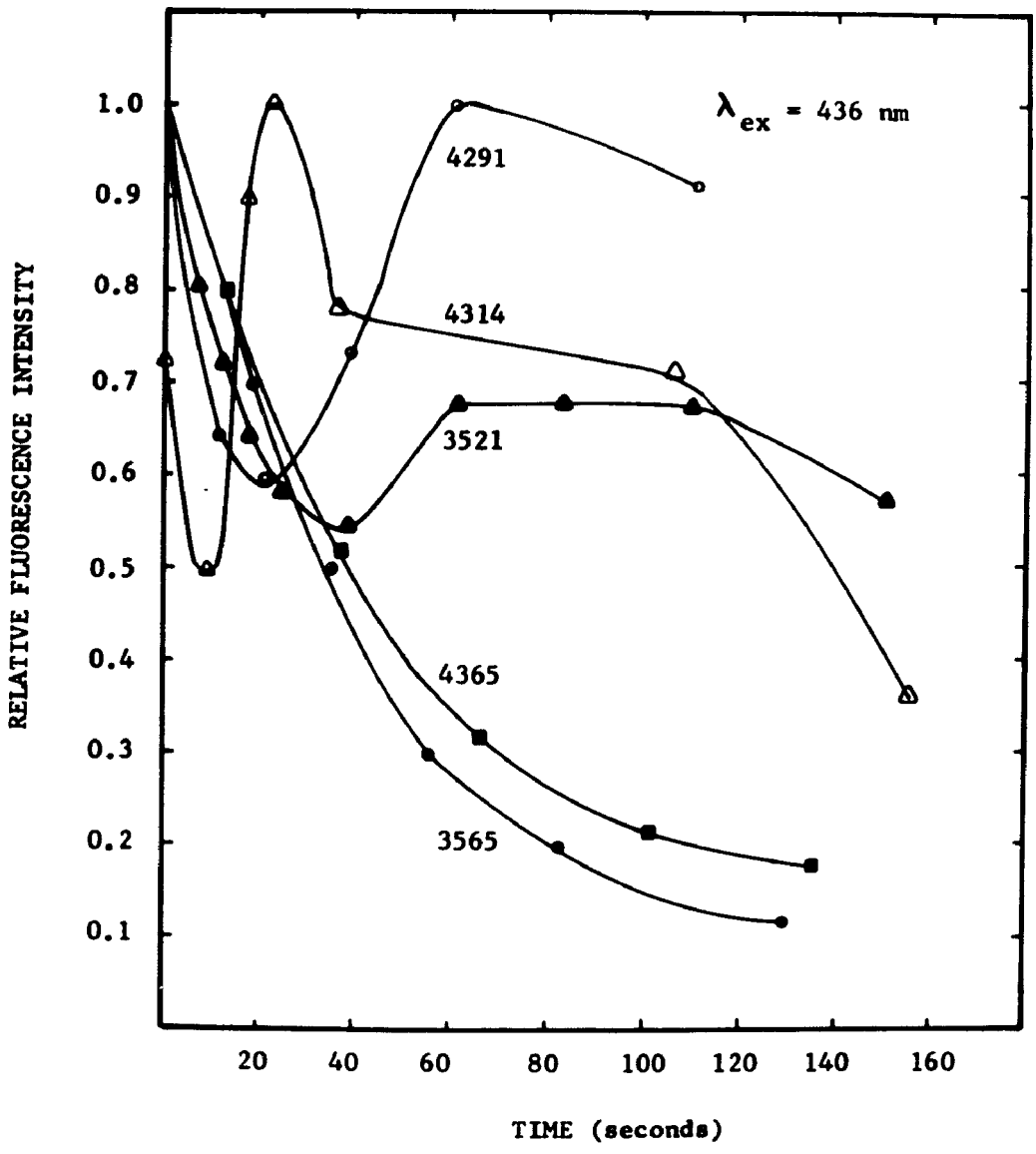
RELATIVE FLUORESCENCE INTENSITY
1.0
0.9
0.8
0.7
0.6
0.5
0.4
0.3
0.2
0.1
20
40
60
80
100
120
140
160
TIME (seconds)
λex = 436 nm
4291
4314
3521
4365
3565

fluorescence emission to increase after the initial decrease, and the build-up in emission can be less, greater, or equivalent to the initial intensity. The fading curve of the cell containing 1.37×10^{-14} mole AO in Figure 24 shows that the fluorescence intensity after the build-up remained fairly constant for approximately 1 min and then decreased. However, for most cells, the increase in emission was immediately followed by a decrease in emission.

Visual observation indicated there was no migration of the dye within the cell during the period of measurement.

Granules in situ. Figure 27 is an example of raw data, a photograph of the oscilloscope display of fluorescence intensity measured at 660 nm over a 20 sec interval. Figure 28 shows the experimental data of Figure 27 expressed in terms of ppu and is representative of the fading behavior of cytoplasmic fluorescence. For most cells, a plot of reciprocal fluorescence intensity as a function of irradiation time yielded a straight line for approximately 12 to 15 sec, after which time the fading reaction deviated from its initial behavior. However, some cells exhibited linear behavior over the entire time of measurement (Figure 29).

Figure 30 is a histogram of 44 slopes taken from plots of reciprocal fluorescence intensity versus time; these slopes are corrected for I_{ex} (slope/I_{ex}). Figure 31 shows the distribution in slopes when the slope values in Figure 30 are normalized with respect to initial fluorescence intensity. The normalized slope is given by multiplying the slope by the initial fluorescence intensity.

FIGURE 27

Oscilloscope display of fluorescence intensity at 660 nm of mast cell granules *in situ* as a function of irradiation time.

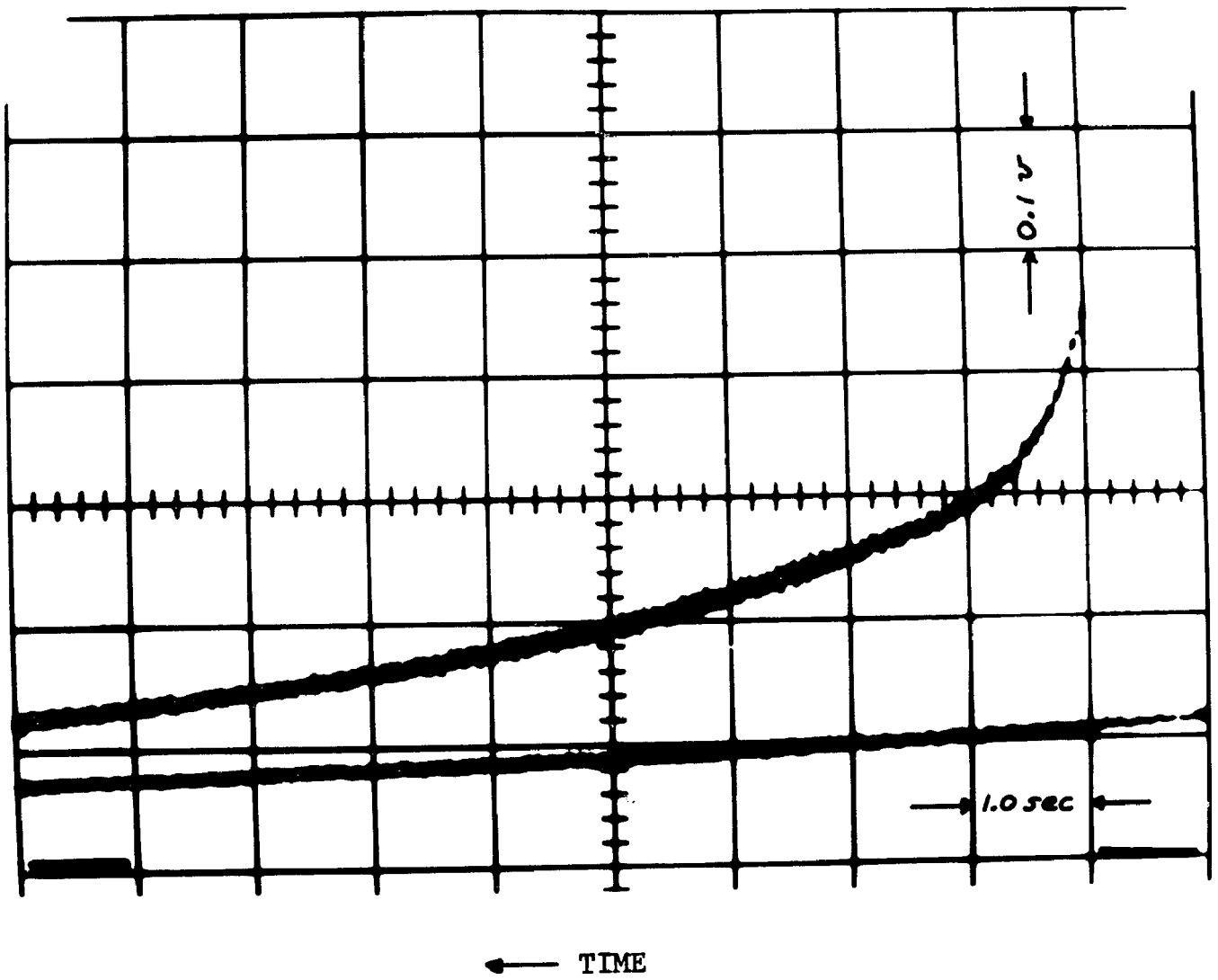
0.1 v
1.0 sec
TIME

FIGURE 28

Fluorescence intensity changes measured at 660 nm of mast cell cytoplasmic granules *in situ*.

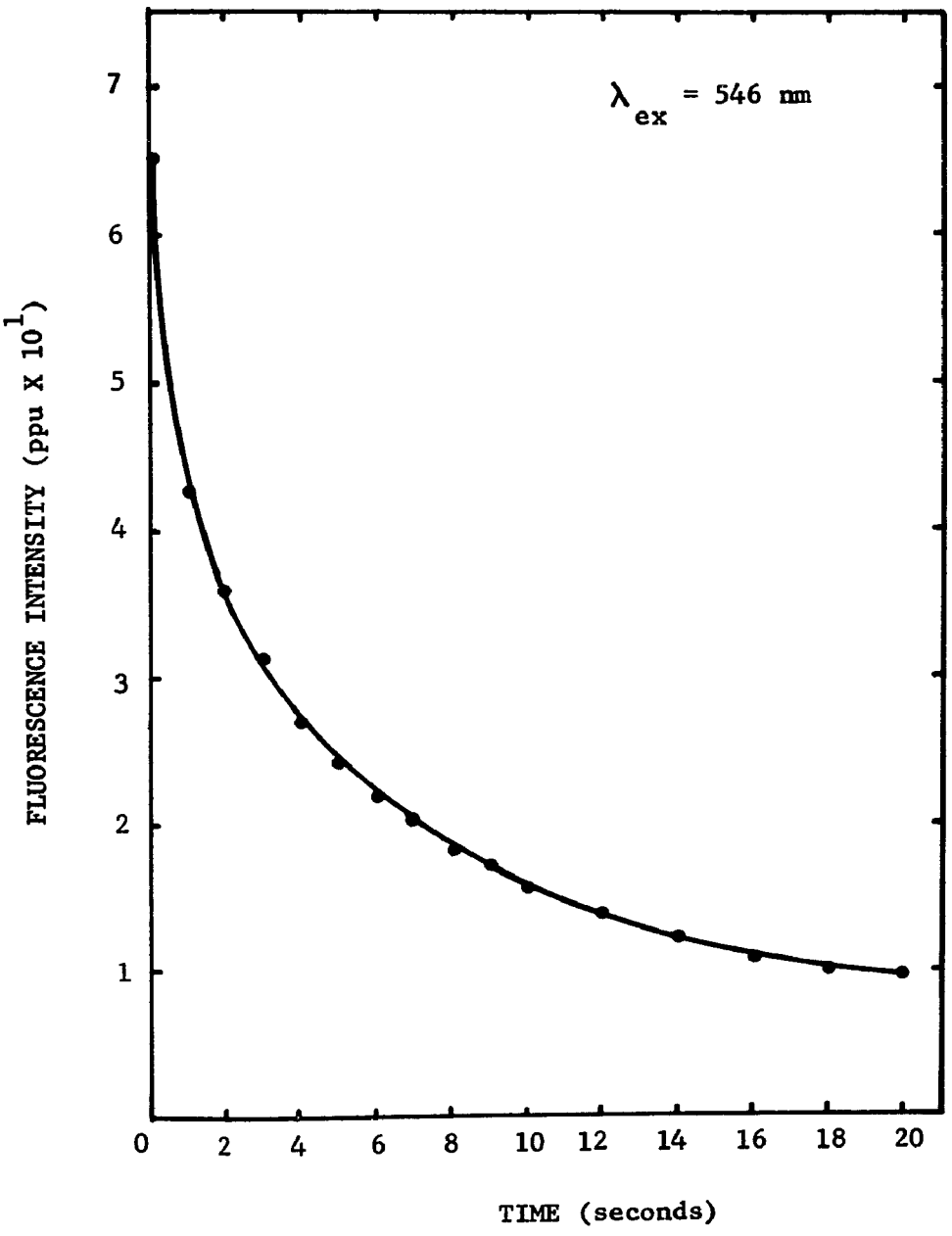
λ_{ex} = 546 nm
FLUORESCENCE INTENSITY (ppu X 10^{-1})
7
6
5
4
3
2
1
0
2
4
6
8
10
12
14
16
18
20
TIME (seconds)

FIGURE 29

Reciprocal fluorescence intensity measured at 660 nm of mast cell cytoplasmic granules *in situ*.

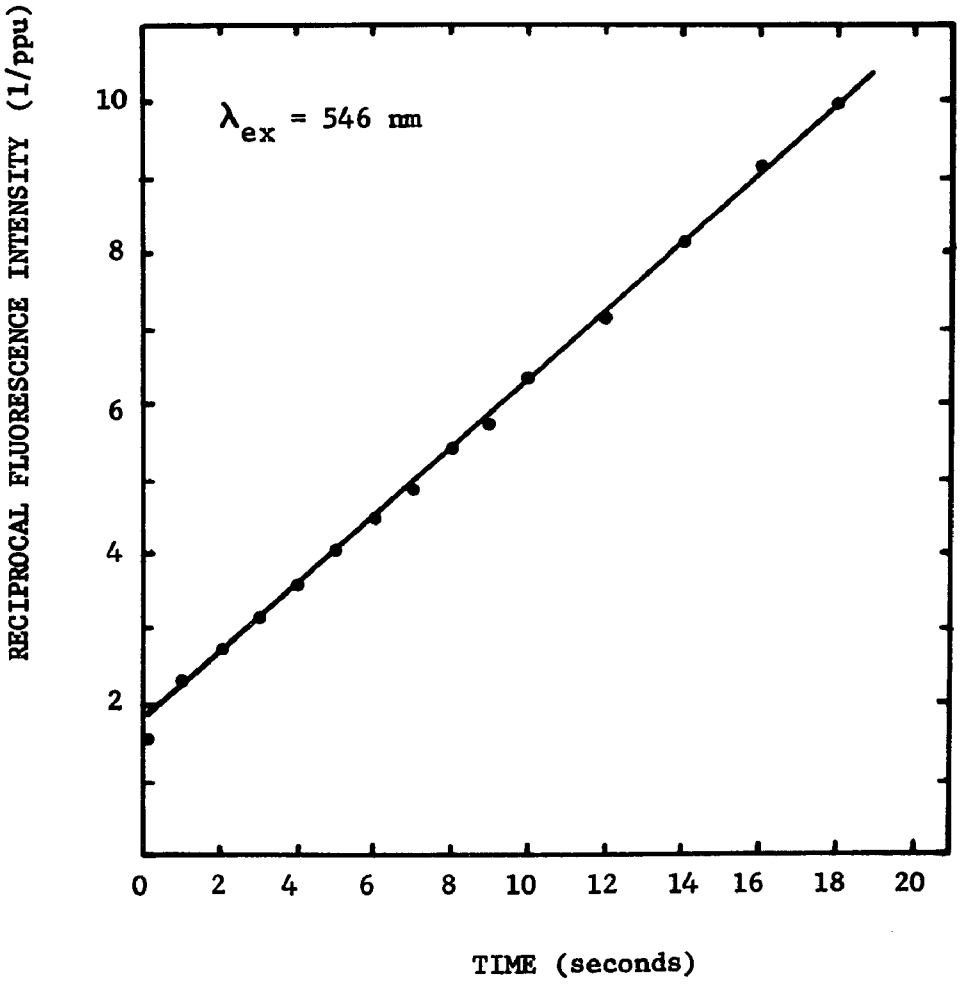
RECIPROCAL FLUORESCENCE INTENSITY (1/ppu)
λ_{ex} = 546 nm
10
8
6
4
2
0
2
4
6
8
10
12
14
16
18
20
TIME (seconds)

FIGURE 30

Distribution of slope values, normalized with respect to exciting light intensity, taken from plots of reciprocal fluorescence intensity at 660 nm versus time for granules *in situ*.

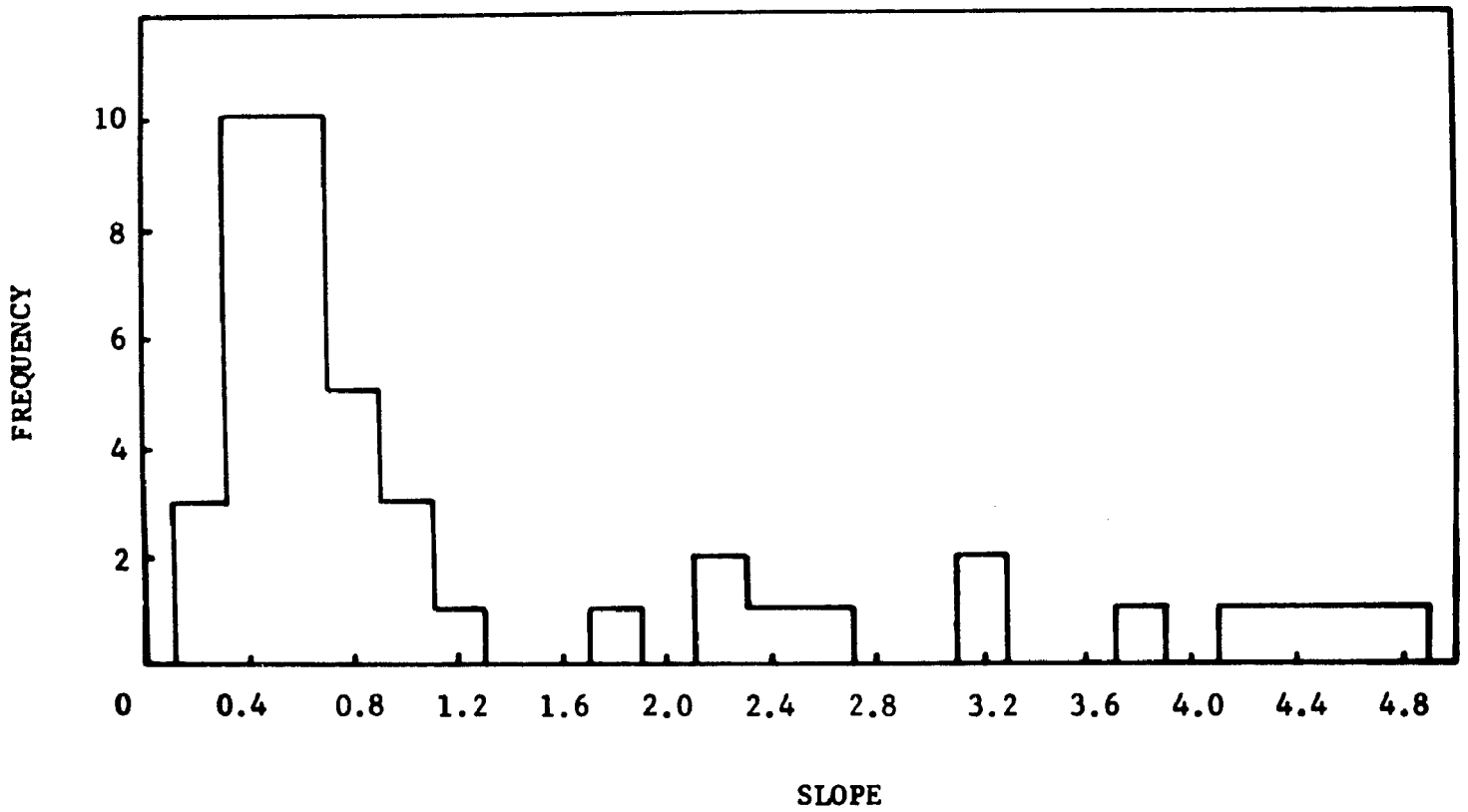
FREQUENCY
10
8
6
4
2
0
0.4
0.8
1.2
1.6
2.0
2.4
2.8
3.2
3.6
4.0
4.4
4.8
SLOPE

Isolated Granule. Single isolated granules exhibited fading behavior similar to that of granules in situ in that a plot of reciprocal fluorescence intensity versus time of irradiation displays a linear relationship (Figure 32). The linear behavior was observed for approximately the first 5 sec in which time there was a 20-30% decrease in the initial fluorescence intensity. The variability in fading behavior among granules is shown in Figures 33 and 34.

Electrophoretic Identification of the AO-AMPS Complexes in MC Granules

Electrophoretic separations indicated that heparin is the only AMPS present in normal rat peritoneal MC granules.

Electrophoretic patterns on two cellulose acetate strips are shown in Figure 35. One strip was stained with alcian blue, commonly used to stain AMPS on cellulose acetate, and the other strip was stained with AO. Electrophoretic migration produced only one band from the sample, and that component traveled the same distance as reference heparin. All components in the granule preparation did not migrate as was evidenced by staining of the strip at the point of sample application.

FIGURE 31

Distribution of slope values of Figure 30 that are normalized with respect to initial fluorescence intensity.

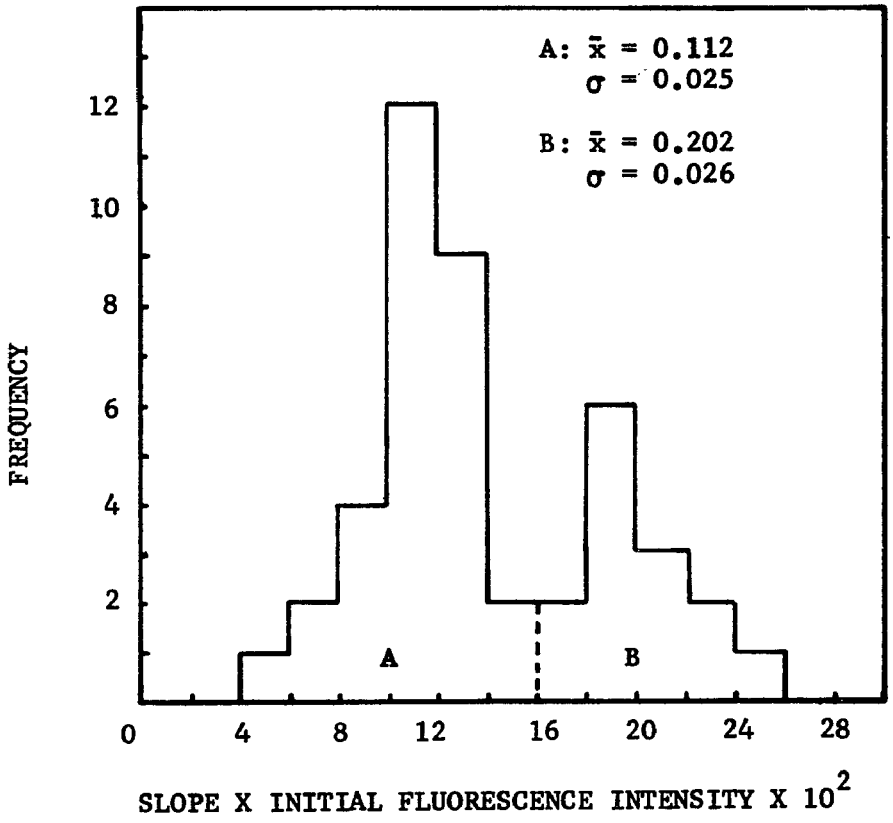
A: $\bar{x}$ = 0.112
σ = 0.025
B: $\bar{x}$ = 0.202
σ = 0.026
FREQUENCY
12
10
8
6
4
2
0
4
8
12
16
20
24
28
A
B
SLOPE X INITIAL FLUORESCENCE INTENSITY X 10^2

FIGURE 32

Reciprocal fluorescence intensity at 660 nm of a single mast cell cytoplasmic granule.

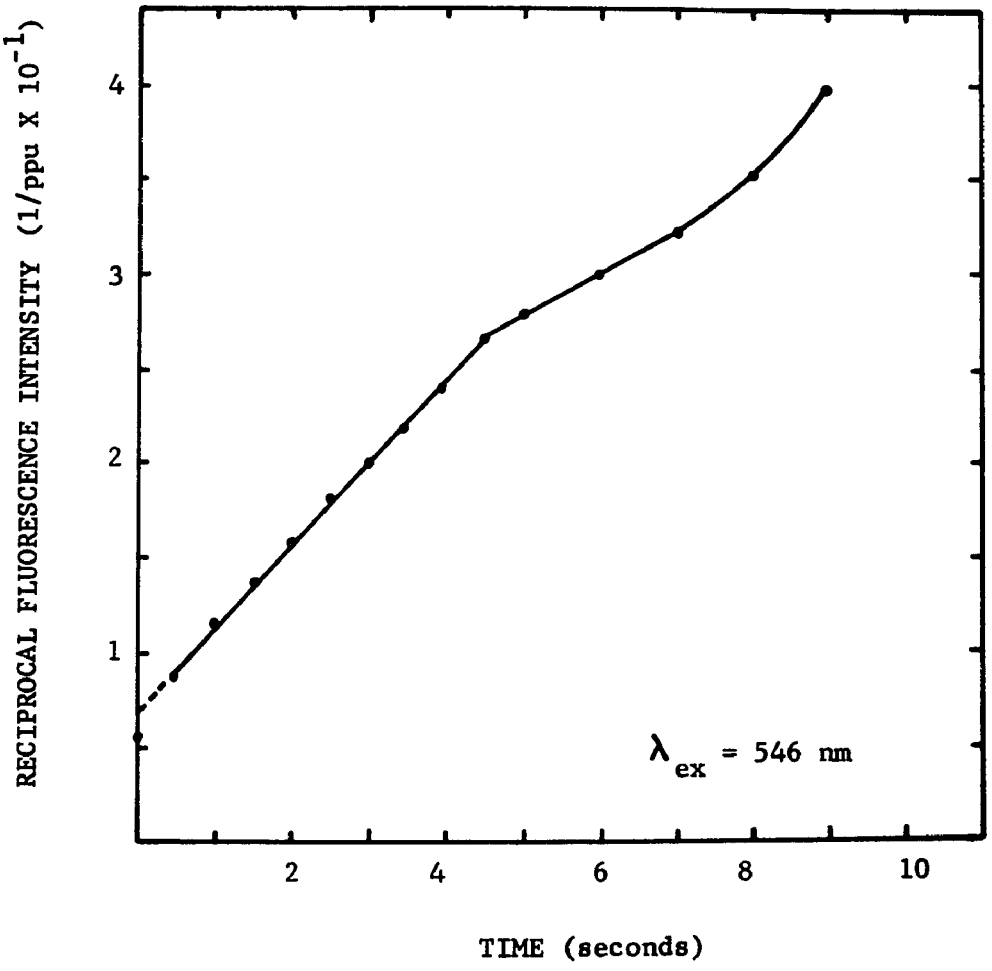
RECIPROCAL FLUORESCENCE INTENSITY (1/ppu X 10^{-1})
4
3
2
1
λ_{ex} = 546 nm
2
4
6
8
10
TIME (seconds)

FIGURE 33

Distribution of slope values, normalized with respect to exciting light intensity, taken from plots of reciprocal fluorescence intensity at 660 nm versus time for single isolated granules.

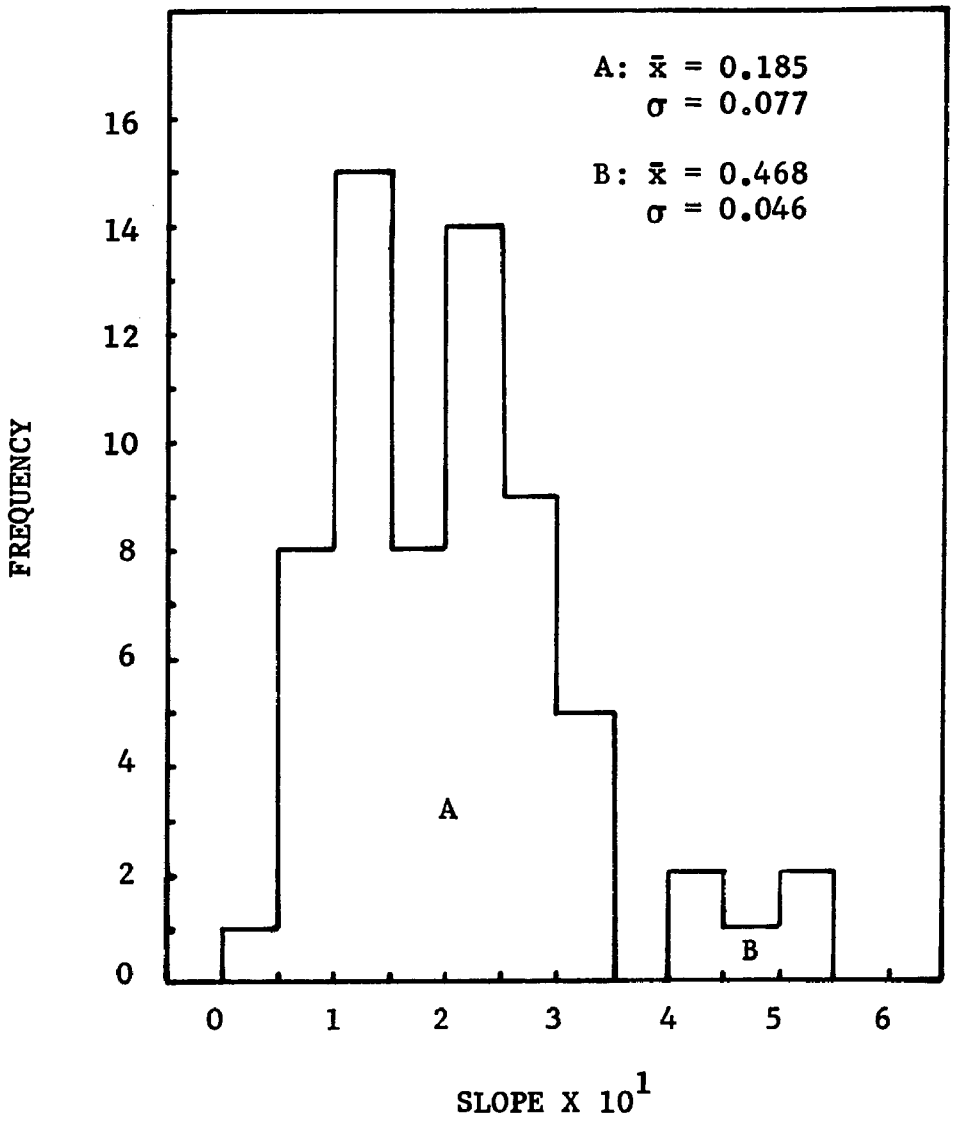
A: $\bar{x}$ = 0.185
σ = 0.077
B: $\bar{x}$ = 0.468
σ = 0.046
FREQUENCY
16
14
12
10
8
6
4
2
0
A
B
0
1
2
3
4
5
6
SLOPE X 10^1

FIGURE 34

Distribution of slope values of Figure 33 that are normalized with respect to initial fluorescence intensity.

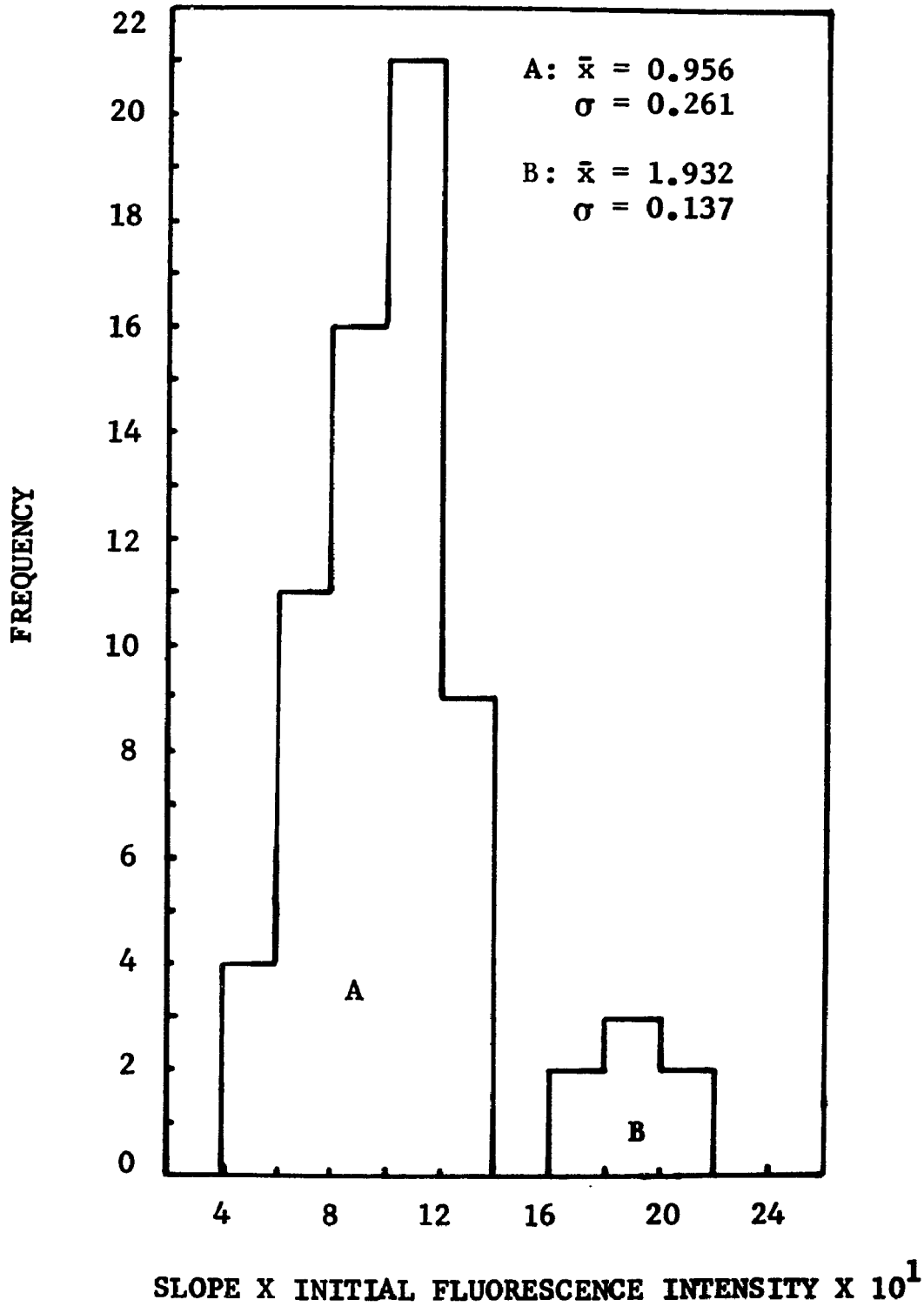
22
20
18
16
14
12
10
8
6
4
2
0
FREQUENCY
A: $\bar{x}$ = 0.956
σ = 0.261
B: $\bar{x}$ = 1.932
σ = 0.137
A
B
4
8
12
16
20
24
SLOPE X INITIAL FLUORESCENCE INTENSITY X 10^1

FIGURE 35

Electrophoresis in cellulose acetate at pH 3. Migration is from bottom to top. Dots at the bottom of each strip are the points of application. Left strip: 100 volts applied for 2 hours; stained with alcian blue. Right strip: 100 volts applied for 1.5 hours; stained with acridine orange. S, mast cell cytoplasmic granule preparation; H, heparin; HS, heparan sulfate; A, chondroitin 4-sulfate; B, dermatan sulfate.

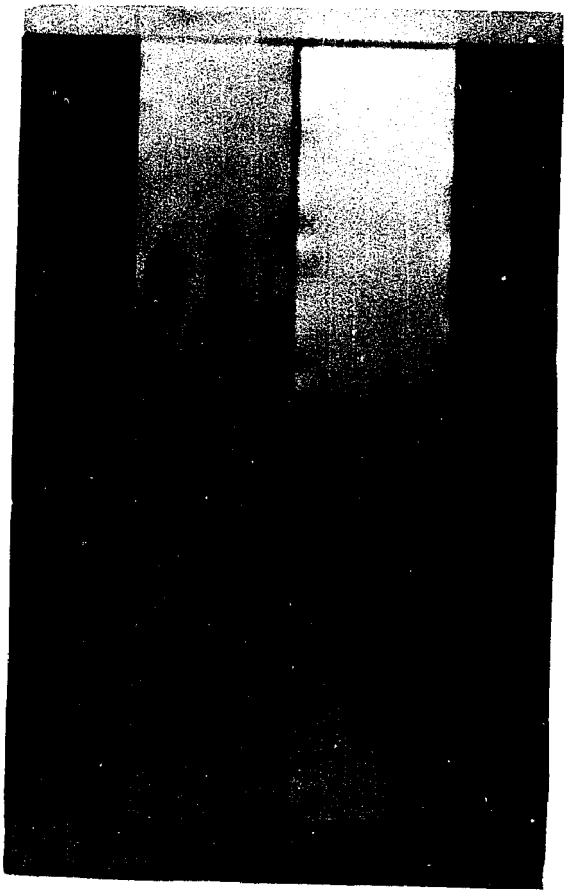

DISCUSSION

Visual observation of fluorescence staining of the mast cell (MC) showed acridine orange (AO) to bind with the nucleus and cytoplasmic granules. AO forms complexes with acid mucopolysaccharides (AMPS), and electrophoretic observation suggested heparin to be the only AMPS present in the granule and the substrate to which AO was bound.

Figure 36 compares equilibrium binding behavior of the MC with that of the normal leukocyte and Ehrlich's hyperdiploid mouse ascites (EHD) tumor cell (West, 1965; Golden and West, 1974). West concluded that over the linear portion of the curve nucleic acid was the primary binding substrate in the leukocyte, and a simple mass action binding model permitted him to calculate the free energy of association which is in agreement with dye-nucleic acid complex in solution (Ichimura et al., 1969). The dye uptake curve of the MC differs markedly in shape from those of other cells in Figure 36 and suggests a different kind of binding.

Figure 8 shows a Scatchard plot of the binding data. A single set of equivalent independent sites produces a linear Scatchard plot; indeed, not the case for the MC. Intuitively, one would not predict a linear plot because visual examination revealed that AO complexed with more than one type intracellular component.

FIGURE 36

Average AO uptake by rat peritoneal mast cells, mouse leukocytes, and Ehrlich's hyperdiploid mouse ascites (EHD) tumor cells as a function of equilibrium free dye available per cell.

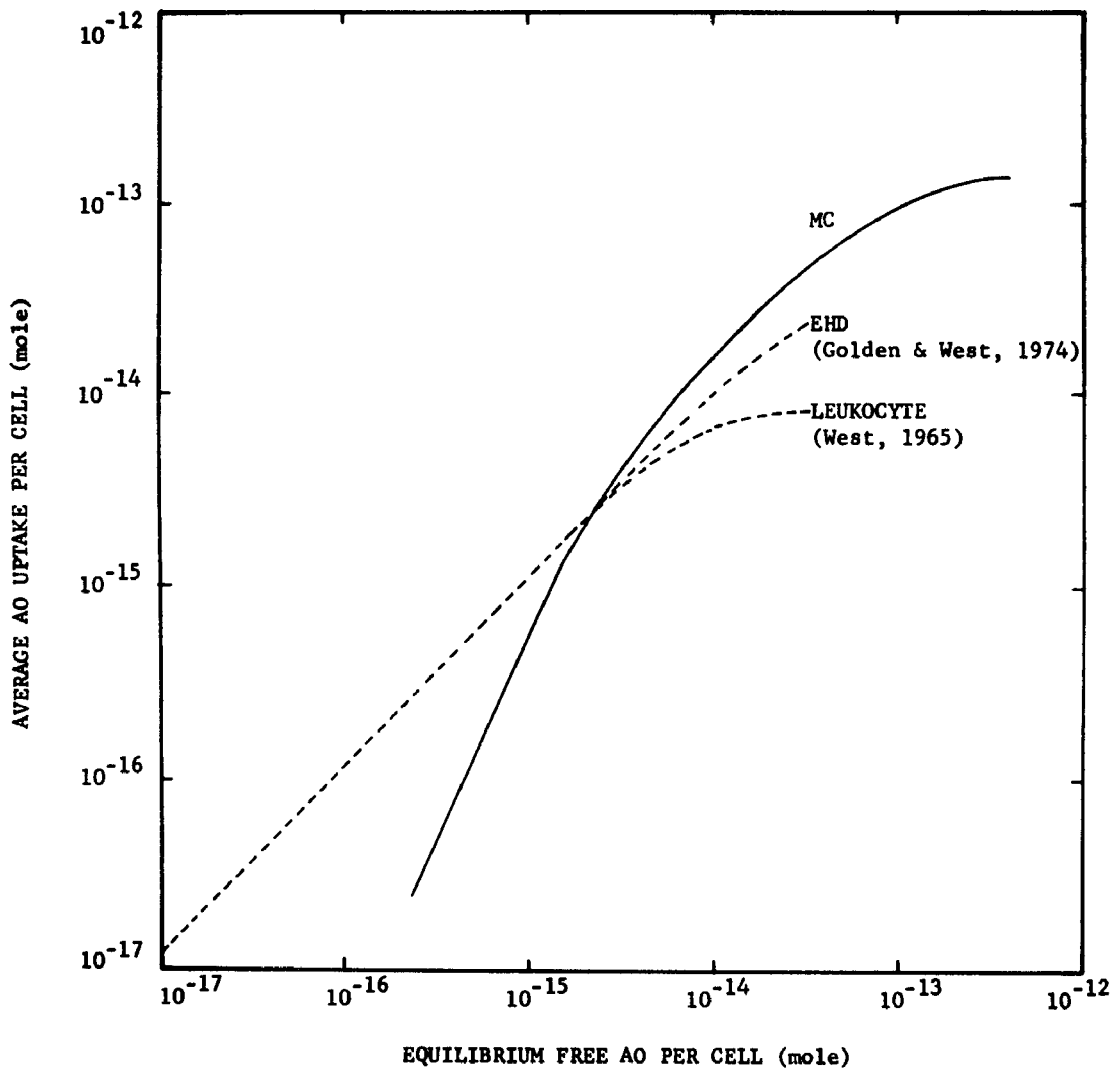
10^{-12}
10^{-13}
10^{-14}
10^{-15}
10^{-16}
10^{-17}
AVERAGE AO UPTAKE PER CELL (mole)
MC
EHD
(Golden & West, 1974)
LEUKOCYTE
(West, 1965)
10^{-17}
10^{-16}
10^{-15}
10^{-14}
10^{-13}
10^{-12}
EQUILIBRIUM FREE AO PER CELL (mole)

Figure 8 is informative, however, because it demonstrates the presence of interaction between nearest sites which promotes positive cooperative binding (Gulati, 1973). Cooperative binding also has been observed in AO-AMPS in solution (Hurst, pers comm).

The MC appears to approach saturation with an average uptake of approximately 1.4 X 10^{-13} mole AO (Figure 7). This value is consistent with what is known about the number of available intracellular anionic sites. Mammalian cells contain approximately 6 pg of DNA (Swift, 1955). On the basis of 6 pg DNA per cell, West (1969) calculated the total number of nucleic acid (DNA + RNA) phosphorus binding sites to be 2.52 X 10^{-14} mole per cell. Assuming all AO taken up by the MC was bound to nucleic acids and heparin, of the 1.4 X 10^{-13} mole AO required for saturation, a maximum of 2.52 X 10^{-14} mole was associated with nucleic acid and the remainder, 1.15 X 10^{-13} mole, complexed with heparin. In 1960, Bloom studied the polysaccharides of the normal rat peritoneal MC and estimated that it contains an average of 20 pg of heparin (Selye, 1965). For that amount of heparin, 1.15 X 10^{-13} mole AO is equivalent to 3.5 anionic sites per disaccharide repeat unit (mol wt = 600).

Lagunoff (1974) investigated the binding of AO with fractions of isolated MC granules and with heparin prepared from the granule. He found 2.53 AO binding sites per disaccharide repeat unit of heparin in the isolated granule and 3.36 sites in heparin prepared from the granule; he postulated that the difference observed in binding could result from the involvement of O-sulfate groups in binding granule protein.

One should keep in mind there is always some indeterminancy in binding values of a particular intracellular component when whole cells are utilized because of the inability to account for the fate of all dye taken up by the cell. Some of the AO taken up by the MC might have been in the form of free dye or complexed with intracellular constituents in addition to heparin and nucleic acids.

Although the number of anionic sites per heparin repeat unit determined by this study is somewhat greater than that reported by Lagunoff for isolated granules, it is in agreement with the total number of binding sites suggested for heparin (Figure 1). The 3.5 acidic groups per repeat unit also is in accordance with the proposed model of heparin-protein binding in which the end of a heparin chain is bound covalently to protein by a galactosylxylosylserine linkage (Lindahl et al., 1965; Lindahl and Rodén, 1965). Serafini-Fracassini and co-workers (1969) concluded from the results of their morphological study on the substructure of the rat MC granule, using electron microscopy, that heparin chains extend laterally from a terminal connection to a central protein "core", which further corroborates the model of Lindahl and colleagues. The number of anionic sites per heparin repeat unit determined by the present study indicates the O-sulphate groups of heparin are not implicated to the extent suggested by Lagunoff in heparin-protein binding.

Two distinct emission bands were observed in spectra of AO stained MCs. One band had an emission maximum centered around 535 nm, the other at 670 nm. The shorter wavelength band was

produced by AO monomer and the longer wavelength red emission resulted when the dye molecules were crowded together on the binding substrate causing dye-dye interaction. The fluorescence spectrum of cell 4622, containing 1.65 X 10^{-16} mole AO, exhibited a green emission peak at 530 nm (Figure 16). With increasing amounts of intracellular dye, slight spectral shifts were observed in this peak which were attributed to the influence of the spectral band centered around 670 nm. The long wavelength emission band in other types of AO-stained cells (e.g., human and mouse leukocytes, EHD tumor cells, and cultured fibroblast) is centered around 660 nm. The different spectral position of the red fluorescence emission peak in the MC was attributed to the AO-heparin complex in the cytoplasm, because an emission maximum at 670 nm also was representative of the red spectroscopic species of AO-heparin complex in solution (Menter, pers comm).

An interesting feature of the AO-MC complex, compared with other cell types that have been quantitatively stained and similarly characterized with fluorescence spectra, is the ability of the MC to demonstrate the presence of the red-fluorescing species with relatively small quantities of intracellular dye. The leukocyte is estimated to contain 2.52 X 10^{-14} mole nucleic acid phosphorus, the AO binding site. The total number of anionic sites estimated for the MC is equivalent to 1.4 X 10^{-13} mole AO. Phosphate moieties are thought to have an orderly arrangement along the DNA molecules (Watson and Crick, 1953). Since AO appears to bind simultaneously to cytoplasmic granules and the nucleus in the MC, one might predict

dye-dye interaction of the bound complex at much lower dye concentrations in the leukocyte relative to the MC, provided the dye is uniformly distributed among the anionic sites. This was not found to occur, however; the red spectroscopic species in the granule was observed at concentrations as low as 5×10^{-16} mole per cell, approximately one decade lower than required to produce red nuclear fluorescence in the mouse leukocyte. These observations indicate a cooperative binding mechanism and stacking of dye molecules among the intragranular polyanion in a manner similar to that described by Bradley and Wolf (1959) for the AO-heparin complex in solution.

The metachromatic behavior of the fluorescing species in the AO-stained MC is reflected in Figures 20 and 21. A log log plot of the ratio of fluorescence intensity at 670 nm to that at 535 nm versus AO uptake per cell is a straight line with a slope of 0.77 (Figure 21). With increasing amounts of intracellular dye, the exponential increase in this ratio nm resulted from dye-dye interaction promoted by the intracellular environment of the dye. The capacity of the intracellular environment to promote dye-dye interaction may be uniquely characteristic of the particular cell type and the intracellular dye binding substrate. However, data in this form are not available on other types of cells.

Although fluorescence fading of AO-polymer complexes with continuous fluorescence-excitation has been recognized for years, not much is understood about the photochemistry of the phenomenon. Figure 26 shows the relative intensity of emission at 535 nm measured of whole cells as a function of time. The spectra of cells

4365 and 3565 consisted primarily of the emission band centered around 535 nm and showed a continuous decrease in fluorescence intensity during the time of measurement. However, cells 3521, 4314, and 4291 which contained both the red and green spectroscopic species demonstrated an initial decrease in emission, followed by an increase, and, finally, a decrease in fluorescence intensity. A wide variation in fading behavior existed among cells taken from the same staining population, and those curves shown in Figure 26 should not be considered representative of all cells containing the amounts of dye indicated.

Variation in fluorescence intensity as a function of irradiation time of the intracellular species having an emission maximum at 670 nm described a smooth function (Figure 25). No buildup in fluorescence was observed, only a continuous decrease in intensity. For these reasons, it was thought that by recording the fading behavior at 660 nm from cell volumes selected to contain granules, some of the difficulties inherent in dealing with the more complex inhomogeneous system of the intact cell would be reduced in studying the fading phenomenon.

Figure 29 shows that a plot of reciprocal fluorescence intensity versus time describes a linear function which suggests that fading proceeds according to a second order reaction, equation 5. The fading of fluorescence at 660 nm in AO-stained MC granules is thought to result from a photochemical reaction between aggregated

ground state AO molecules, A, and aggregated excited state molecules, A^*, given by

$$A + A^* \xrightarrow{k} P \qquad (1)$$

where P is the reaction product. The rate of the reaction can be described by

$$\frac{-d\,[A]}{dt} = k\,[A]\,[A^*] \qquad (2)$$

where k is the second order rate constant.

For dilute dye solutions, a linear relationship exists between [A] and $[A^*]$. Therefore, equation (2) can be written in terms of A given by

$$\frac{-d\,[A]}{dt} = k'\,[A]^2 \qquad (3)$$

which on integration yields

$$\frac{1}{[A_t]} = k't + \frac{1}{[A_o]} \qquad (4)$$

where $[A_t]$ is the concentration of A at time t, $[A_o]$ is the initial concentration of A, and k' is the apparent rate constant which is proportional to k. Replacing concentration with fluorescence intensity, I_f, yields

$$\frac{1}{I_{ft}} = k_f' t + \frac{1}{I_{fo}} \qquad (5)$$

where I_{ft} is the fluorescence intensity at time t, I_{fo} is the initial fluorescence intensity, and k_f' is a constant proportional to the second order rate constant for fluorescence.

Because the fluorescence fading reaction of the AO-granule complex <u>in situ</u> followed second order kinetics, it was thought that

a k_f' value unique for the complex could be determined. However, slopes taken from plots of $1/I_f$ versus t and normalized with respect to I_{ex} showed much variability (Figure 31). Solution studies (Menter, pers comm) and other cell studies (Golden and West, 1974) have demonstrated fading rate is proportional to I_{ex}.

Cytoplasmic fluorescence which had a higher I_{fo} value also tended to have a lower k_f' value. When the k_f' values were multiplied by I_{fo}, better coincidence was obtained. This normalization for I_{fo} gave a continuous distribution of slopes in this sample. When this type of normalization for I_{fo} was applied to fading data obtained from different concentrations of AO-AMPS in solution, a single slope, a constant proportional to the second order rate constant, resulted. A corrected slope, k", can be defined as

$$k'' = k_f' I_{fo}/I_{ex} \qquad (6)$$

It was thought that perhaps intercellular differences in the geometrical arrangement of granules within the cytoplasm were manifest in different fading rates. Therefore, it was decided to study the fading behavior in the single isolated granule. The results of the fluorescence fading studies on isolated granules were different from those expected. The fading was faster and also produced a wider range of k" values than was found for granules in situ.

The reason for the greater fading rate of the isolated granule compared with granules in situ is not understood. Perhaps sonication which was used to disrupt the cell in making granule preparations, the extracellular environment, or the high level of staining

that was required for measurable fluorescence altered the granule's molecular conformation which may play a role in the fluorescence fading process. Based on the fading characteristics of granules both in situ and isolated, there appear to be two populations of granules. The fading curve slopes of granules in situ are centered around k" = 0.11 and k" = 0.20; for the single isolated granules, the k" values group around k" = 0.96 and k" = 1.9 (Figures 31 and 34).

It would be interesting to determine if the two types of MC granules observed at the electron microscope level are the same as those differentiated by fluorescence fading. If the different k" values result from different fluorescing complexes that are characteristic of the two types of granules, these experiments demonstrate that the slopes of fluorescence fading curves might serve to identify biopolymers in situ.

Occasionally, $1/I_f$ versus time plots for both the single isolated granule and granules in situ could be described with two straight lines. Since the first straight line always had a greater slope, one might speculate that two photochemical reactions occurred simultaneously at first, and later one reaction stopped while the other reaction continued. This would account for the second slope always being less than the first slope which would then represent the sum of two second order reactions. Alternatively, two consecutive second order reactions could also yield a similar result.

An equation* has been derived (Menter, pers comm) to describe the second order fading behavior of the red spectroscopic species of AO-biopolymer complexes in dilute solution and is given by

$$1/I_{ft} = \Phi_{rx}/\Phi_f \, A \cdot t + 1/I_{fo} \qquad (7)$$

where Φ_{rx} is the quantum efficiency of the reaction(s) responsible for the disappearance of AO, and Φ_f is the quantum efficiency of fluorescence. The slope, $\Phi_{rx}/\Phi_f C$, of equation (7) corresponds to k_f' of equation (5). Equation (7) does describe the fluorescence fading data. Additional experiments are needed to completely evaluate the various factors included in the slope of the equation, the derivation of which was for dilute solution, to determine their applicability to fluorescence fading kinetics in cell systems.

At the present time no chemical model is available which satisfactorily explains the photochemical events evidenced by fluorescence fading in cells. It is speculated, however, that some type of photochemical reaction between excited and ground state dye molecules bound along the polymer chain yields a non-fluorescing reaction product, the nature of which is unknown. When more is understood about the basic nature of the AO-complex and the various parameters which affect the intracellular fading process, perhaps physical-chemical data derived from fluorescence fading measurements can be properly interpreted and provide useful information about AO-intracellular complexes.

---

* A manuscript giving the derivation of equation (6) is in preparation.

CONCLUSIONS AND RECOMMENDATIONS FOR FUTURE WORK

The work presented in this dissertation establishes the facts that AO binds to heparin in the unfixed MC and that the AO-heparin complex can be qualitatively and quantitatively studied by physical optical and physical chemical means. The optical properties of the AO-heparin intragranular complex are altered as a function of intracellular dye content. AO-staining of the MC is not limited to cytoplasmic granules, other cell organelles (e.g., the nucleus and nucleolus) also form complexes with AO.

The following conclusions and recommendations for future work result from this investigation of the interaction of AO with the peritoneal MC of the rat.

Conclusions

(1) The results of the equilibrium binding studies between AO and the MC differed markedly from those obtained with other cell types (e.g., leukocytes and EHD tumor cells). The difference in shape of the dye uptake curve is attributed to cooperative interaction between the binding sites of heparin, the primary dye binding substrate in the MC.

(2) Fluorescence microscopy of the AO-stained MC yields spectra with distinct emission peaks at approximately 535 nm and/or

670 nm. The intensity of fluorescence and the shape of the spectrum are functions of the amount of dye taken up by the cell. The spectral position of the long wavelength peak is different than that observed in other cell types but is in agreement with solution studies of the AO-heparin complex, leading to the conclusion that AO binds to heparin in the MC.

(3) Fluorescence fading of the 670 nm fluorescence band of the AO-MC granule complex follows second order reaction kinetics.

(4) Based on the fluorescence fading curve slope, k", of the AO-stained MC granules, there appear to be two populations of granules with the larger population having the slower fading rate.

(5) The ratio of fluorescence intensity at 670 nm to that at 535 nm of the AO-stained MC is a function of the quantity of intracellular dye raised to the 0.77 power. This function is indicative of the capacity of the cell to promote dye-dye interaction and may be uniquely characteristic of a particular cell type and the intracellular dye binding substrate(s).

Recommendations for Future Work

(1) Conduct equilibrium binding studies between AO and polymers of known conformation and composition containing only one type of binding site (e.g., phosphate, sulphate, or carboxyl groups). Fluorescence fading studies on these chemically defined complexes would also be useful in determining if fading behavior is uniquely characteristic of a particular AO binding substrate.

(2) Determine if other cell types and *in vitro* model systems each promote dye-dye interaction, with increasing quantities of bound dye, in a characteristic manner evidenced by the change in the ratio of fluorescence intensity of the longer wavelength to that of the shorter wavelength emission band.

(3) Determine if experimental or intrinsic factors are responsible for the difference in fading rate between granules *in situ* and the single isolated granule.

(4) Determine if tumor MCs can be differentiated from normal MCs by the methodology used in this investigation.

(5) Obtain optical rotatory dispersion (ORD) data on supravitally stained MCs. ORD spectra could provide insight as to the nature of the dye-polymer complexes and could be especially informative when correlated with other optical properties of the complexes.

SIGNIFICANCE

Methodology has been presented here for staining heparin in physiologically competent MCs and for making qualitative and quantitative measurements on the AO-heparin complex within individual cells. The physical chemical data obtained on the identified intracellular complex can be directly correlated with *in vitro* solution data on the AO-heparin complex. Therefore, the nondestructive methods can be of fundamental importance in gaining insight into the physiological role of heparin in the MC. This work establishes a basis for future cytochemical and biochemical experiments that can utilize the behavior of the dye in dealing with both normal and pathological processes of the cell where heparin is, or might be, involved (e.g., synthesis, catalysis, response to pharmacological agents, etc.).

BIBLIOGRAPHY

Åborg, C.-H., Novotný, J., and Uvnäs, B. Ionic binding of histamine in mast cell granules. Acta Physiol. Scand. 69, 276-283 (1967).

Åborg, C.-H., and Uvnäs, B. Mode of binding of histamine and some other biogenic amines to a protomine-heparin complex in vitro. Acta Physiol. Scand. 74, 552-567 (1968).

Asboe-Hansen, G. The origin of synovial mucin. Ann. Rheum. Dis. 8, 149-157 (1949).

Barker, S. A., Cruickshank, C. N. D., and Webb, T. Mucopolysaccharides in mouse skin. Part I. Isolation and identification. Carbohyd. Res. 1, 52-61 (1965a).

Barker, S. A., Cruickshank, C. N. D., and Webb, T. Mucopolysaccharides in mouse skin. Part II. Characterization of a novel sulphated nucleotide. Carbohyd. Res. 1, 62-70 (1965b).

Barrnett, R. J., Hagen, P., and Lee, F. L. Mast cell granules containing 5-hydroxytryptamine, histamine and heparin morphologically and biochemically distinct from mitochondria. Biochem. J. 69, 36 P (1958).

Benditt, E. P. Morphology, chemistry, and function of mast cells. Ann. N. Y. Acad. Sci. 73, 204-211 (1958).

Benditt, E. P., Wong, R. L., Arase, M., and Roeper, E. 5-Hydroxytryptamine in mast cells. Proc. Soc. Exp. Biol. 90, 303-304 (1955).

Bergendorff, A., and Uvnäs, B. Storage of 5-hydroxytryptamine in rat mast cells. Evidence for an ionic binding to carboxyl groups in a granule heparin-protein complex. Acta Physiol. Scand. 84, 320-321 (1972).

Bertalanffy, L. von. Acridine orange fluorescence in cell physiology, cytochemistry, and medicine. Protoplasma 57, 51-83 (1963).

Bloom, G., and Ringertz, N. R. Acid polysaccharides of peritoneal mast cells of the rat and mouse. Arkiv. Kemi. 16, 51-56 (1960).

Bradley, D. F., and Wolf, M. K. Aggregation of dyes bound to polyanions. Proc. Natl. Acad. Sci. 45, 944-952 (1959).

Brunish, R., and Asboe-Hansen, G. Acid mucopolysaccharides in the Rask-Nielsen transplantable mouse mastocytoma. Acta Path. Microbiol. Scand. 65, 185-191 (1965).

Cass, R., Riley, J. F., West, G. B., Head, K. W., and Stroud, S. W. Heparin and histamine in mast-cell tumors from dogs. Nature 174, 318-319 (1954).

Cifonelli, J. A., and Dorfman, A. The uronic acid of heparin. Biochem. Biophys. Res. Commun. 7, 41-45 (1962).

DeBruyn, P. P. H., Robertson, R. C., and Farr, R. S. In vivo affinity of diaminoacridines for nuclei. Anat. Rec. 108, 279-304 (1950).

Ehrlich, P. Contributions to the theory and practice of histological staining, Inag. Diss. University of Leipzig (1878). In The Collected Papers of Paul Ehrlich, Vol 1, F. Himmelweit, ed. Permagon Press, New York (1956).

Fullmer, H. M. Differences in mechanism in staining reactions for mast cells. Nature 183, 1274-1275 (1959).

Golden, J. F., and West, S. S. Fluorescence spectroscopic fading behavior of Ehrlich's hyperdiploid mouse ascites tumor cells supravitally stained with acridine orange. J. Hist. Cyto. 22, 495-505 (1974).

Graham, H. T., Lowry, O. H., Wahl, N., and Priebat, M. K. Mast cells as sources of tissue histamine. J. Exp. Med. 102, 307-318 (1955).

Gulati, J. Cooperative interaction of external calcium, sodium, and oubain with the cellular potassium in smooth muscle. Ann. N. Y. Acad. Sci. 204, 337-357 (1973).

Hagen, P., Barrnett, R. J., and Lee, F. L. Biochemical and electron microscopic study of particles isolated from mastocytoma cells. J. Pharmacol. Exp. Ther. 126, 91-97 (1959).

Helting, T. and Lindahl, U. Occurrence and biosynthesis of B-glucuronidic linkages in heparin. J. Biol. Chem. 246, 5442-5447 (1971).

Herd, J. K. Identification of acid mucopolysaccharides by microelectrophoresis. Analyt. Biochem. 23, 117-121 (1968).

Hill, R. B., Bensch, K. G., and King, D. W. Unimpaired mitosis in cells with modified deoxyribonucleic acid. Nature 184, 1429-1430 (1959).

Hodgman, C. D. Handbook of Chemistry and Physics, 36th ed. Chemical Rubber Publishing Co., Cleveland (1954).

Horsfield, G. I. Mast cell mucopolysaccharides. Nature 211, 422 (1966).

Horsfield, G. I., and Summerly, R. Mucopolysaccharides in mast cells. Brit. J. Derm. 78, 476-484 (1966).

Ichimura, S., Zama, M., Fujita, H., and Ito, T. The nature of strong binding between acridine orange and deoxyribonucleic acid as revealed by equilibrium dialysis and thermal renaturation. Biochim. Biophys. Acta 190, 116-125 (1969).

Jancsó, N., Jancsó-Gábor, A., and Balassy, J. A method for in vitro investigation of the colloid-storing function of histocytes. Nature 184, 1070-1071 (1959).

Jorpes, J. E. Heparin in the Treatment of Thrombosis. Oxford University Press, London (1946).

Korn, E. E. The synthesis of heparin in mouse mast cell tumor slices. J. Am. Chem. Soc. 80, 1520-1521 (1958).

Lagunoff, D. Round table discussion. J. Padawer, ed. Ann. N. Y. Acad. Sci. 103, 441-490 (1963).

Lagunoff, D. The mechanism of histamine release from mast cells. Biochem. Pharmacol. 21, 1889-1896 (1972).

Lagunoff, D. Analysis of dye binding sites in mast cells. Biochem. 13, 3982-3986 (1974).

Lagunoff, D., Phillips, M. T., Iseri, O. A., and Benditt, E. P. Isolation and preliminary characterization of rat mast cell granules. Lab. Invest. 13, 1331-1344 (1964).

Lindahl, U. The structures of xylosylserine and galactosylxylosylserine from heparin. Biochim. Biophys. Acta 130, 361-367 (1966).

Lindahl, U., Cifonelli, J. A., Lindahl, B., and Rodén, L. The role of serine in the linkage of heparin to protein. J. Biol. Chem. 240, 2817-2820 (1965).

Lindahl, U. and Rodén, L. The role of galactose and xylose in the linkage of heparin to protein. J. Biol. Chem. 240, 2821-2826 (1965).

Loeser, C. N., and West, S. S. Cytochemical studies and quantitative television fluorescence and absorption spectroscopy. Ann. N. Y. Acad. Sci. 97, 346-357 (1962).

Loeser, C. N., West, S. S., and Schoenberg, M. C. Absorption and fluorescence studies on biological systems: nucleic acid-dye complexes. Anat. Rec. 138, 163-178 (1960).

Magnusson, S. and Larsson, B. Uptake of ^{35}S-labelled sulfate in the heparin of dog mastocytoma. Acta Chem. Scand. 9, 534-535 (1955).

Michels, N. A. The mast cells. In Downey's Handbook of Hematology, Vol. 1. Hoeber, New York, pp 232-272 (1938).

Mota, I., Ferri, A. G., and Yoneda, S. The distribution of mast cells in the digestive tract of laboratory animals: its bearing on the problem of the localization of histamine in tissues. Quart. J. Micr. Sci. 97, 251-256 (1956).

Oliver, J., Bloom, F., and Mangieri, C. On the origin of heparin. An examination on the heparin content and specific cytoplasmic particles of neoplastic mast cells. J. Exp. Med. 86, 107-123 (1947).

Padawer, J. Mucopolysaccharides of normal mast cells. Amer. J. Anat. 127, 159-179 (1970).

Price, G. P., and Schwartz, S. Fluorescence microscopy. In Physical Techniques in Biological Research, Vol III, G. Oster and A. W. Pollister, eds. Academic Press, New York (1956).

Riley, J. F. Histamine in tissue mast cells. Science 118, 332-333 (1953).

Riley, J. F. The Mast Cells. Livingstone, Edinburgh (1959).

Riley, J. F. and West, G. B. The presence of histamine in tissue mast cells. J. Physiol. (London) 120, 528-537 (1953).

Ringertz, N. R. Acid polysaccharides of two mast cell tumors in mice. Acta Chem. Scand. 14, 312-320 (1960).

Scatchard, G. The attraction of proteins for small molecules and ions. Ann. N. Y. Acad. Sci. 51, 660-672 (1949).

Schayer, R. W. Formation and binding of histamine by free mast cells of rat peritoneal fluid. Am. J. Physiol. 186, 199-202 (1956).

Schiller, S., and Dorfman, A. The isolation of heparin from rat mast cells of the normal rat. Biochem. Biophys. Acta 31, 278-280 (1959).

Schubert, M., and Hamerman, D. Metachromasis: chemical theory and histochemical use. J. Histochem. Cytochem. 4, 159-189 (1956).

Selye, H. The Mast Cells. Butterworth, London (1965).

Serafini-Fracassini, A., Durward, J. J., and Crawford, J. The morphology of the heparin-protein macromolecule and its organization in the mast cell granule. J. Ultrastruct. Res. 28, 131-140 (1969).

Steiner, R. F., and Beers, R. F. Polynucleotides. V. Titration and spectrophotometric studies upon the interaction of synthetic polynucleotides with various dyes. Arch. Biochem. Biophys. 81, 75-92 (1959).

Swift, H. Cytochemical techniques for nucleic acids. In The Nucleic Acids, E. Chargaff and J. N. Davidson, eds. Academic Press, New York (1955).

Uvnäs, B., Åborg, C.-H., and Bergendorff, A. Storage of histamine in mast cells. Evidence for an ionic binding of histamine to protein carboxyls in the granule heparin-protein complex. Acta Physiol. Scand. 78, Suppl. 336, 3-26 (1970).

Velican, C., and Velican, D. Histochemical investigations on the presence of hyaluronic acid in mast cells. Acta Haemat. 21, 109-117 (1959).

Watson, J. D., and Crick, F. H. Molecular structure of nucleic acids. Nature 171, 737-738 (1953).

West, S. S. Fluorescence microspectroscopy of mouse leukocytes supravitally stained with acridine orange. In Methoden und Ergebnisse der Zytophotometric, W. Sandritter and G. Kiefer, eds. Acta Histochem., Suppl. 6, 135-153 (1965).

West, S. S. Fluorescence microspectrophotometry of supravitally stained cells. In Physical Techniques in Biological Research, Vol 3c, A. W. Pollister, ed. Academic Press, New York (1969).

West, S. S. Optical rotatory dispersion and the microscope. In Introduction to Quantitative Cytochemistry, Vol II, G. L. Wied and G. F. Bahr, eds. Academic Press, New York (1970).

Winkelmann, R. K. Orthochromatic, species-limited staining of mast cells with night blue. Stain Tech. 34, 227-231 (1959).

Worthington, W. C., and Bailey, N. C. Dual staining of mast cell cytoplasmic constituents by alcian blue and safranin. J. Hist. Cyto. 10, 503 (1962).

GRADUATE SCHOOL
UNIVERSITY OF ALABAMA IN BIRMINGHAM
DISSERTATION APPROVAL FORM

Name of Candidate Larry D. Love

Major Subject Physiology and Biophysics

Title of Dissertation A Study of the Interaction of Acridine Orange with Rat Mast Cells

Dissertation Committee:

__________, Chairman

Director of Graduate Program __________

Dean, UAB Graduate School __________

Date Nov. 7, 1975